Investigation on Laser Assisted Post Processing of Wire Arc Additive Manufacturing of NiTi Shape Memory Alloys

M. Tech Thesis

by

Vinod Singh Thakur

(1702103007)

Department of Mechanical Engineering

Indian Institute of Technology Indore

JUNE 2019

Investigation on Laser Assisted Post Processing of Wire Arc Additive Manufacturing of NiTi Shape Memory Alloys

A THESIS

Submitted in partial fulfilment of the

requirements for the award of the degree

of

Master of Technology

in

Mechanical Engineering

With specialization in

Production and Industrial Engineering

by

Vinod Singh Thakur

Department of Mechanical Engineering

Indian Institute of Technology Indore

JUNE 2019

Indian Institute of Technology Indore

Candidate's Declaration

I hereby certify that work which is being presented in the thesis entitled **Investigation on Laser Assisted Post Processing of Wire Arc Additive Manufacturing of NiTi** in the partial fulfilment of the requirements for the award of the degree of **MASTER OF TECHNOLOGY** and submitted in the **DISCIPLINE OF MECHANICAL ENGINEERING, Indian Institute of Technology Indore,** is an authentic record of my own work carried out during the time period July 2017 to June 2019 under the supervision of **Dr. I.A. Palani**, Head, Discipline of Mechanical Engineering, Indian Institute of Technology Indore.

The matter contained in this thesis has not been submitted by me for the award of any degree from any other institute.

Vinod Singh Thakur

(1702103007)

This is to certify that the above statement made by the candidate is correct to the best of our knowledge.

(Dr. I.A. Palani)

Vinod Singh Thakur has successfully completed his M.Tech Oral Examination held on…………

Signature of the Thesis Supervisors
Date:

Signature of Convener, DPGC
Date:

Signature of the PSPC Member 1
Date:

Signature of the PSPC Member2
Date:

Acknowledgement

I take this opportunity to express my deep sense of respect and gratitude for, Dr. I.A. Palani, for believing in me to carry out this work under his supervision. His constant encouragement, friendly interactions, and constructive support have enabled this work to achieve its present form. His innovative perspective towards things and his continuous pursuit for perfection has had a profound effect on me and has transformed me majorly. I feel greatly privileged to be one of his students.

I also express my sincere thanks to Sophisticated Instrumentation Centre (SIC), IIT Indore for providing me with the necessary characterization facility throughout my research period.

I am thankful to IIT Indore for giving me an opportunity to carry out the research work and providing all the facilities. Very special thanks to Prof. Pradeep Mathur, Director, IIT Indore, for supporting and providing us facilities to perform my work smoothly here.

I am extremely thankful to Mr. S.S. Mani Prabu, Mrs. Ankita Sahu for guiding and helping me out from the very first day I joined this project. I would also like to express my thanks to M. Manikandan and all members of Opto-Mechatronics group for their moral support and the friendly nature we have created in our lab.

Lastly, but undoubtedly the most valued, gratitude is expressed for my parents, for letting me choose my dreams and supporting me endlessly. Your un-matched support made this work possible.

Vinod Singh Thakur

Dedicated

to

My family

And

My Friends

Abstract

Additive manufacturing (AM) the process of joining materials to make parts or objects from 3D model data, basically layer over layer deposition, as to prevent to subtractive manufacturing technology. In my work wire, arc additive manufacturing (WAAM) technique is used for the fabrication of the metal parts as the workpiece, that is based on the principle of the metal inert gas (MIG) welding. Shape memory alloys (SMA's) is the alloys, which exhibit two unique properties such as pseudo-elasticity and the shape memory effect (SME). SMA’s alloyed metal that can sustain a large amount of deformation, through heating it will return to their original shape or heating above the austenite temperature. SMA’s have applications in robotics and automotive, aerospace and biomedical industries.

This paper shows the experiments performed on WAAM fabricated NiTi bulk structure which was cut through the wire EDM and then after first performed the laser diffusion over copper coated NiTi and second the laser annealing of the NiTi thin strip sample.

The investigation over the WAAM fabricated NiTi bulk structure has been done. After this characterization have been done by using a scanning electron microscope, optical microscope, micro-hardness, x-ray diffraction and composition analysis by using energy dispersive x-ray spectroscopy and phase transformation by using differential scanning calorimeter. And for shape memory effect by using hot plate actuation.

List of Publications

Papers in Conference Proceedings

- **Vinod Singh Thakur**, Manikandan M, I.A. Palani, "Investigations on Laser assisted shock peening of the untwined NiTi to shape memory alloy structures using solid-state nanosecond Nd: YAG laser," *DAE-BRNS National Laser Symposium (NLS-27), 2018.*
- **Vinod Singh Thakur**, Manikandan M, Shalini Singh, Shivam Mishra, Ankit Kaithwas, Mani Prabu S, I.A. Palani, "Laser polishing of Wire Arc Additive Manufactured SS 316L," 7th International & 28th AIMTDR Conferences, 2018.
- Sahu, Ankita; S. S., Mani Prabu; N, JINOOP; M, Manikandan; **Thakur, Vinod Singh**; Palani, I; C.P, Paul; K. S., Bindra "Investigations on phase transformation and shape memory characteristics of NiTi using Wire arc based additive manufacturing technique" Journal of Intelligent Material Systems and Structures. [Communicated]

Table of content

List of the figures

List of the table

Acronyms

WAAM	Wire arc additive manufacturing
AM	Additive manufacturing
SMA	Shape memory alloy
SME	Shape memory effect
EDM	Electrical discharge machining
MSMA	Magnetic shape memory alloy
A_s	Austenite start
A_f	Austenite finish
M_s	Martensite start
M_f	Martensite finish
OWSME	One-way shape memory effect
TWSME	Two-way shape memory effect
DSC	Differential scanning calorimeter
XRD	X-Ray diffraction
SEM	Scanning Electron Microscope
EDS	Energy Dispersive X-Ray Spectroscopy.

Chapter 1

Introduction

1.1 Shape Memory Alloys (SMAs)

Advanced engineering alloys or smart material also known as memory alloys. Normally alloys mean the combination of the two or more alloys, it has been preparing to enhance the properties and to gain more industrial application. If we take normal alloy when it heated they change their shape when we cooled, they won't become to their original shape but appear to come in a new form. But whereas we take an SMA and when subjected to thermal procedure what happen, they regain their original shape, or they recover their original shape, so this specular property or phenomenon known as shape memory alloys (SMA).

SMA has a wide range of application in industry and medical fields [1]. In an industrial area such as cryofit hydraulic tube coupling for joining the tube, the temperature control system used as switches, and variable register, force actuation to shut off the gases valve due to their temperature variable. In a medical area such as blood clotting filter, eye frame glasses, tumour identification, catheter, and as they have biocompatible property used as a bone plate, and also for hip joint material [1]. There are so many materials found where we observed shape memory effect in many alloys including NiTi, Cu-Al-Ni, Cu-Zn-Al, Cu-Sn, Nb-Ti, Cu-Al-Be and Ti-Nb.

The principle following the SMA actuators is in the translation of heat energy into moving energy and as work output. These actuators give a large amount of motion at low operating voltages. An array of benefits, such as high recoverable forces, different actuation system and give high output work per unit mass or per unit volume, can be achieved by these actuators.

Hence, SMA actuation mechanisms are one of the most preferred actuation mechanisms.

1.2 Phenomenon in SMAs

SMAs alloys have two exclusive phases, the first one is the austenite phase and the second one is the martensite phase. Martensite phase will occur at very low temperature when the material has taken as very low temperature they may undergo the phase named as martensite and where we can see the material is very soft and deformable.

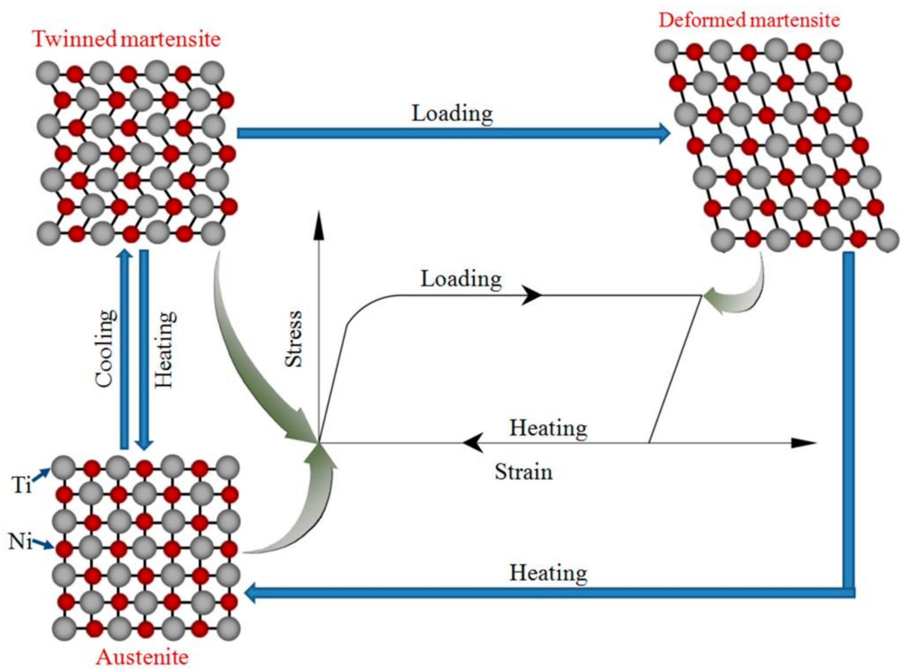

Fig 1.1 Deformation Mechanisms of NiTi Shape Memory Alloy [2]

But the same material undergoing the austenite phase that is when we are increasing the temperature which means that only on happens high temperature, these we can say that material undergoes stronger one. Both are changing their state by heating or cooling process because of an extraordinary property called SMA

1.3 Characteristics of the SMAs

There is some important property of the SMA such as shape memory effect, Pseudoplasticity and hysteresis which are discussed in that section,

Shape Memory Effect (SME)

When we took material, initially material will low temperature (room temperature) it would be in martensitic state (twinned martensitic state), but when we going to apply some load, it changes into another form of state which is known as deformed martensitic state (detwinned martensitic state), when it is heated then martensite is converted into austenite then material would be regain into martensite state. We can say that by changing the temperature transformation is happens to SMAs, So this type of effect known as SME.

Pseudoplasticity

There are Pseudo means false, elasticity means a material which regaining its shape while applying the load or also remove the load. Initially, we have to heat, it changes, or it would be getting transforms to austenite state. But when we have to apply some load over the austenite material. The material gets changed into martensite state, again which the load is removed the material being getting changed into austenite, and we are not at all changing the temperature, this property known as pseudoplasticity.

Hysteresis

In this property as we have seen, the transformation and the temperature changes even know they are happening with a wide range, there is no overlapping of the transformation of temperature happens over here, so when we are put as a graph to get a balanced graph like their hysteresis. by seeing their SME, we are able to say it got a wide range of application in both industry and medical application due to its temperature variation factor.

One-way shape memory effect (OWSME)

One-way shape memory alloys basically when we heated the SMA it will come on their original shape, it means regaining its original shape only on heating alone this phenomenon is known as OWSME.

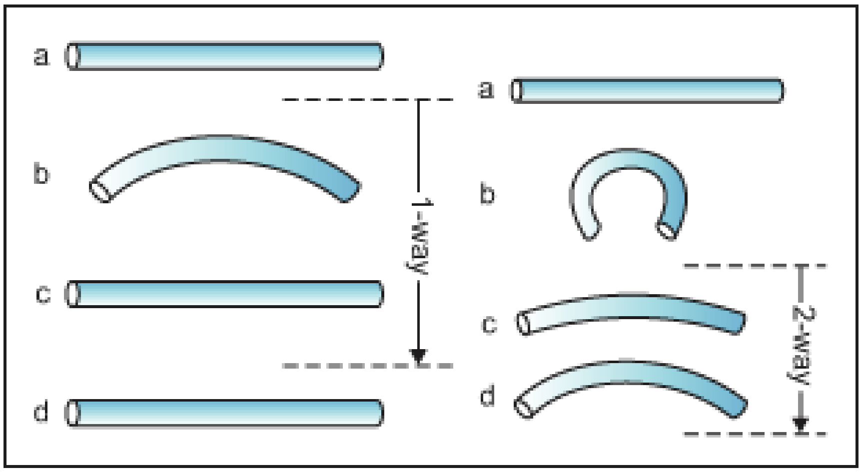

Fig 1.2 Schematic of the OWSME and TWSME (source: creative commons license)

Two-way shape memory effect (TWSME)

When we are heating and cooling the SMAs it will come to their original shape after deforming its shape. It means regaining its shape for both heating and cooling of the process, this phenomenon is known as TWSME.

1.4 Applications of bulk NiTi Shape Memory Alloys

Application of NiTi bulk SMA structures is also of wide scope not only in MEMS but also in vibration absorption and other dampers applications. And also, benefits for the seismic structure design because of the widespread plastic distortion having a huge capacity to absorb energy. Ability to returns to original shape after plastic deformation and allow for deformation while minimizing permanent damage to structural integrity and extend lifetime to serviceability. We can include in the new structure and retrofitting to the existing structure.[3]

Ma HW et al [4] describe the advance SMA-based vibration damper primarily containing pre-tightened highly elastic SMA wires and two recompressed springs as shown in Fig 1.3. effective as energy dissipation, correspondingly. These damper improved energy and high power that dissipate power while strengthen apply by tension SMA wires and roller system [4], though the recompressed springs give the damping force and then after restore that forces.

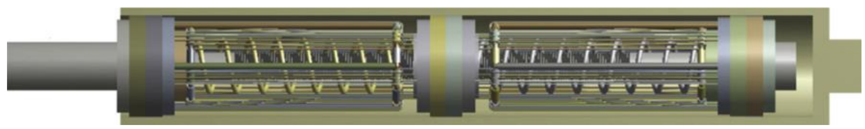

Fig 1.3 schematics of the SMA shock absorber section view

Yang et al [5] that established and estimate the performance of a hybrid seismic device consisting of three important equipment first group of reentering SMA wires, second couple of energy-absorbing struts, and third is a couple of high-strength steel tubes to lead the moving of the hybrid devices Fig 1.4.

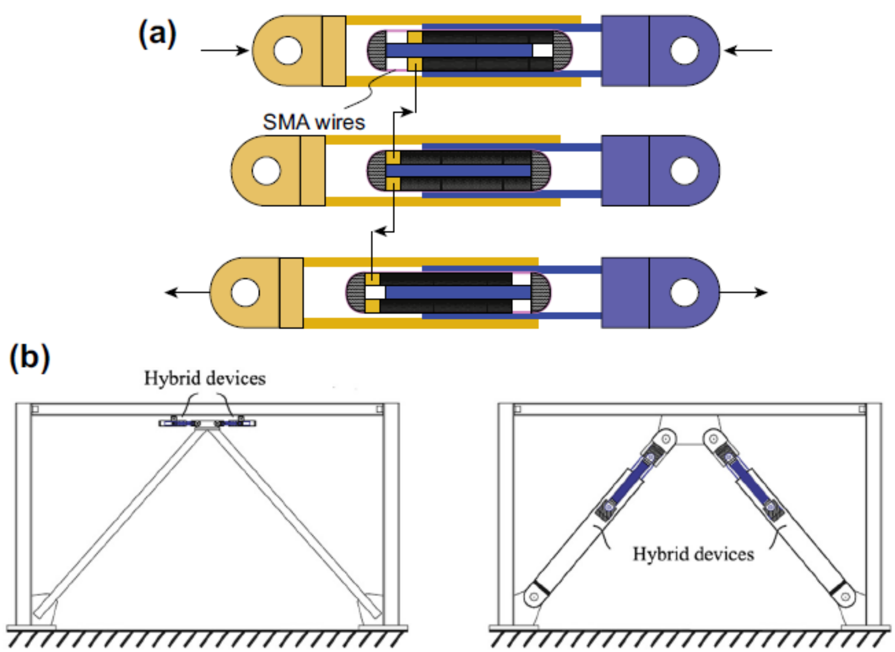

Fig 1.4 (a) Planned SMA hybrid device (b) Distinct conformations planned devices

G. Song et al [6] in these vibration absorption devices which are made of the SMAs and steel rod and wire were installed diagonally in double level steel as shown in Fig.1.5(a). Yu-Lin Han et al [7] They displayed that the planned devices have various characteristics such as good energy consumption, small displacement due to high stiffness and easily working mechanism. Leon et al [5,8] used martensite SMA tendons as the primary load transferring elements in steel beam-column connections Fig.1.5(c).

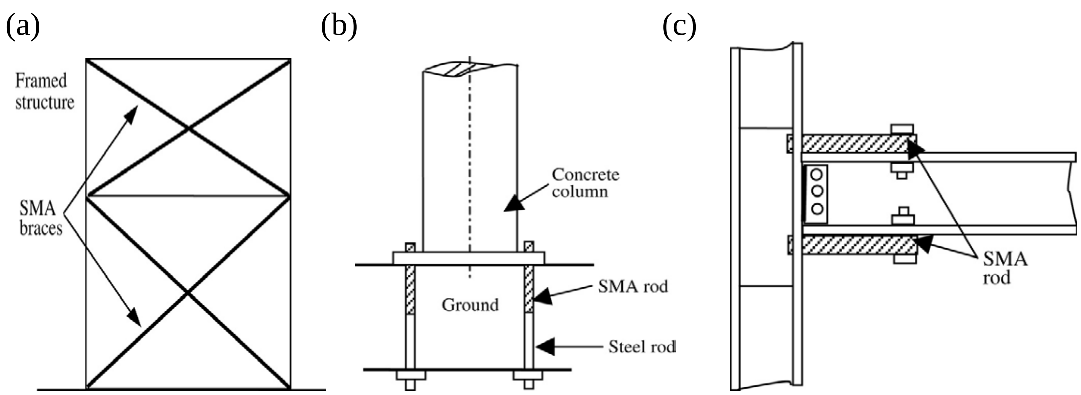

Fig. 1.5 Schematic of (a) SMA braces for double story frame (b) SMA bar as a column, and (c) SMA connector for steel structures

1.5 Objective of the Present Research Work

- Fabrication of NiTi bulk structure using Wire Arc Additive Manufacturing (WAAM) Technique.
- Copper deposition over WAAM fabricated bulk NiTi structure using DC magnetron sputtering.
- Laser diffusion of Copper sputtered NiTi using Solid state nanosecond Nd: YAG laser.
- Laser annealing of WAAM fabricated bulk NiTi structure using Ytterbium-doped fibre Laser.

1.6 Research Methodology

The research methodology used for our process work

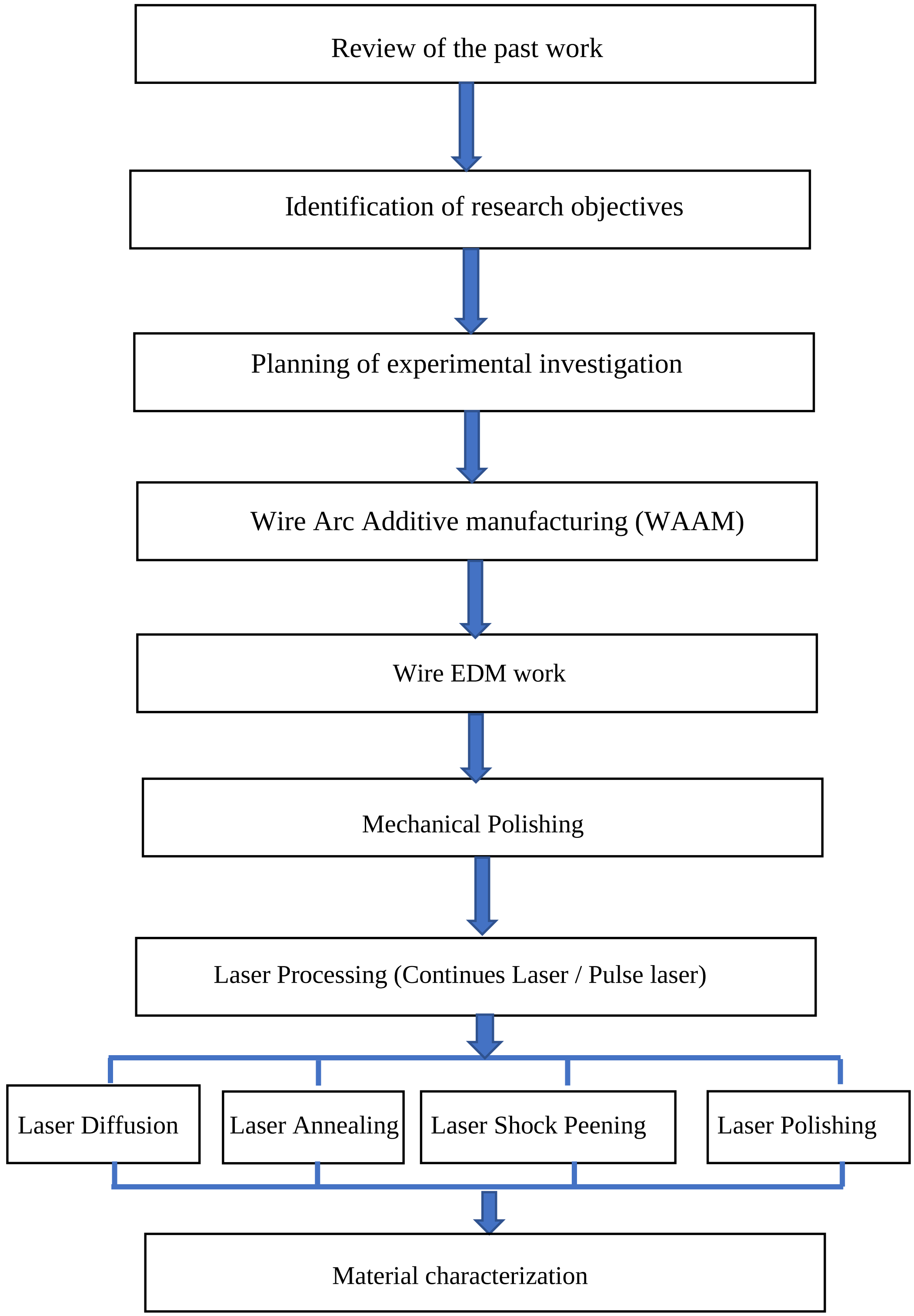

1.7 Outline of the Thesis

Chapter 2 Presents a review of the past work on the additive manufacturing, DC magnetron sputtering for copper deposition, laser diffusion and the laser annealing.

Chapter 3 Discuss the complete description of the experiments of the Additive manufacturing process and their result and discussion.

Chapter 4 Discuss the detailed description of the experiments of the diffusion for which we used DC magnetron sputtering then after laser diffusion and their result and discussion.

Chapter 5 Presents a complete explanation of the laser annealing of a fabricated sample with their procedure their result and discussion, the conclusion of the whole work.

Chapter 6 Discuss the investigations on Laser assisted shock peening of the untwined NiTi SMAs structures.

Chapter 7 In this chapter presents the Laser polishing of Wire Arc Additive Manufactured SS 316L.

Chapter 2: Literature Review

This chapter provides an insight into the methodology and technology available in the additive manufacturing (AM), magnetron sputtering, laser diffusion and the laser annealing. It also highlights various methods used by researchers on this topic. Additive manufacturing is the advanced manufacturing technology that involved both conventional and advanced method with automation system and CNC system research of mechanics and method plays a major role in the research work. manufacturing mechanisms are governed by fusion and deposition which in turn is influenced by welding speed, power, feed rate.

Here we get the feel of the topic by getting to know about various methods and mechanisms governing additive manufacturing, the influence of various parameters on the additive manufacturing operation.

2.1 About the shape memory alloy

Dimitris C. Lagoudas [9,10] This literature discussed the unique property of the SMAs, how is different from the other alloys material. Because of the exceptional characteristic property of the shape memory alloys and associated with the thermal as well as mechanical behaviour discussed in detail, SMAs is the exclusive alloys material which has the capability to change their shape and recovered their original shape due to the enhancement of the temperature. An enhancing the temperature can give the outcome in shape recovery even after the load is applied and applied stress due to the beauty of the SMA behaviour under a given condition. SMA can absorb the shock and the dissipate the energy, therefore, it is used for the vibration absorption application in automobile and the aerospace industry.

D. J. Hartl et al [9] In this literature describe, investigated of the essentials of shape memory alloy behaviours and its characterization which are helpful for the better consideration of the thermo-mechanical response. Moreover, appropriate confirmation of required material property which is helpful for the fabrication and development of the wide-ranging and proper SMA material prototype. Whatsoever technology was used in this section for the development of the SMA further used for their application.

2.2 Past work on additive manufacturing

Seyed Hamidreza Ghaffar et al [11] discussed about the manufacturing and fabrication of the eco-friendly Shape memory alloys using the advance an emerging technology known as additive manufacturing (AM). Through this technology production of the building structure and the digital framework model without any human interaction. However, technological and the advance challenges required to address the industrial execution of additive manufacturing such as material quality, product and production quality, standardization of the production, an interfacial layer of the manufactured material and the deposited layer over the one layer. AM is one of the most innovative keys enabling the method to create an optimized solution for the technologies. These are the decisive relation between material structure and for the manufacturing of the complex 3D geometry of the printing system.

Sajan Kapil et al [12] Here HLM manufacturing technology is used for fabrication of the product. In this section with the help of the HLM software will make an exact geometry of the product geometric data input (3D CAD model). When implemented the geometric program then start slicing the layer, one by one over the other layer, tool follow the tool path and process parameter, with the help of computerized numerical control (CNC) controller. HLM software also manages the motion of the translation stages, power source and the wire feed rate. This experiment is done for obtaining the dimensional accuracy of the product. For this work for the HLM technology, tungsten inert gas (TIG) welding has been studied and developed by TIG cladding process. After fabrication the characterization studied has been done to know the behaviour of the mild steel layer wire.

Fisseha Legesse et al [13] advance layered manufacturing process combines incorporation of additive and subtractive manufacturing processes. This process takes the advantages of both the reduction of the material and the after the product has been fabricated after the material remains. For this hybrid layer fabrication method metal inert gas (MIG) welding is used for the making the model. Initially Before and after making the model they are studies about the simulation and the part feature of the model and after that they made. MIG welding machine for layer has been used for adding the layer and for the deduction of the material computer numerical control milling machine is used and finishing the product.

2.3 Past work on the sputtering

Minh-Tung Le et al [14] In this literature by the DC magnetron sputtering thin layer of the copper deposited over the substrate. By magnetron sputtering in a balanced quantity we can deposit, and we can control the thickness of the deposition that's they used the magnetron sputtering. In this sputtering two different source and target material is used for the layer, from the target to the source one medium is required for moving the sputtered particle known as shielding gas, in this paper argon gas used for the medium with the Cu film deposited over the substrate, is the lower rate of the sputtered power. The growth rate of the thin film of the copper is relating throughput the magnetron sputtering and their nucleation mechanism.

Jin Hyo Boo et al [15] In this paper they have deposited thin layer of the copper (Cu) using DC magnetron sputtering over the silicon Si (100) substrate and glass substrate during the sputtering the growth temperature of the gun between the 573 K to 753 K, this much range they maintained during the deposition and they the planed and design of the high power unstable sputtering for the deposition. This sputtering is more efficient that is five times more than the conservative sputtering method. And they have also improved the ion among the substrate and the source.

2.4 Past work on the actuation

Yves Bellouard et al [16] In this section reviews the several efforts that were completed to present the ideology of the SMA microactuator and the SMA microsystem which are offering the position of the current research and the possible outcome of the progress the research perspective. And they have discussed the several actuation systems such as spring based microsystem, biomorph based microactuator system, SMAs winding around the stick for actuation and microvalve which is also used as an actuator.

S.S. Mani Prabu et al [17] This paper discussed the actuation of the SMAs of the friction stir welding process. In this work, they have performed a solid-state welding method known as friction stir welding. Welding through very high-speed rating the weld around 800 to the 1000 rpm. After that hey cut the welded sample in thin strip shape for performing the actuation operation. And phase conversion behaviour of the welded sample for the different rotating speed by DSC. For the actuation section, they have used the hot plate, in hot plate austenite temperature used for the heated the sample, visibly absorbed thin strip that regains their original shape after heating. And it was found for the entirely recovered angle it took around the 27s.

Chapter 3: Additive Manufacturing

3.1 Background

Additive manufacturing (AM) is an advanced manufacturing process that is most important in industrial applications such as automobile industry, aircraft and aerospace industry. Additive manufacturing is defined as "the process of joining materials to make parts or objects from 3D model data, usually layer upon layer, as opposed to subtractive manufacturing methodologies". An important distinguishing feature of the AM is that by this technique layer by layer deposited over another layer and built up of the part over another layer without specific part tooling and no other external part is required.

3.2 Major classification of the additive manufacturing process

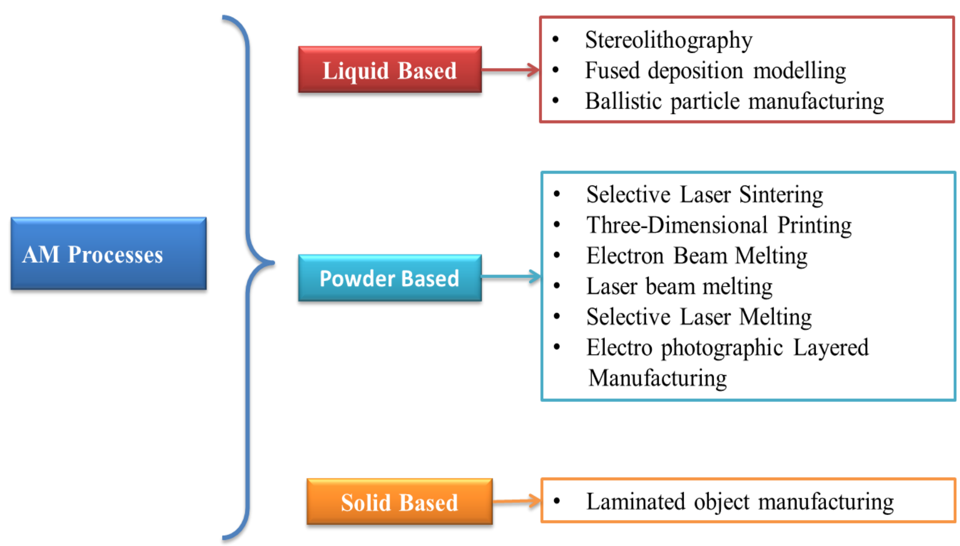

3.3 Principle of AM

WAAM for AM works on the basic principle of fusion and deposition due to electric arc. This electric arc is used for the melt the consumable feed wire as a material which coagulates together and makes a strong stronger layer over the substrate and the argon gases are used for the working medium as a shielding gas with the proper gas flow rate. This makes the good surface finish and a stronger layer of the material [18,19].

AM is an advanced process that makes a promise to reduce product cost by eliminating material depletion and waste time to market [18]. And, the independent of the part feature, AM does not require the blank and it is the full automation and fast process, complex work is done easily [20].

3.4 Wire arc additive manufacturing (WAAM)

AM the process of layer by layer deposited over another layer and built up of the part over another layer without specific part tooling as against the subtractive manufacturing. In my work wire-based arc additive manufacturing (WAAM) technique is used for the fabrication of the metal parts as the workpiece, that is based on the principle of the metal inert gas (MIG) welding.

The binding of an electric arc as fusion and wire as feedstock by wire feeder is WAAM and has been investigating for AM purposes since the 20th century. WAAM is the assembly of the welding power source, torches and wire feeding system and XY stages that provide the motion using the robotic system or robotic arms. With the help of Repitier host software, we made a program on that software using G-code and M-code and then after executing that program to the XY stage. XY stage gave the motion to the x-direction, y-direction and z-direction. wire feeder provided the wire as the feedstock to the welding torch which is connected to the X-Y stage and using welding power source supply the optimized power such as voltage and the wire feed rate to the welding torch during that high energy region plasma was created and then start deposition in the argon environment.

Table 3.1 WAAM process parameter

Sample	Wire feed rate (m/min)	Argon gas flow rate (L/min)	Voltage (V)	Current (A)	Wire diameter (mm)
NiTi	7.5	20	18	197	0.8

With the help of NiTi wire, we are fabricating a bulk structure of the NiTi material by using the WAAM technique. By using the WAAM fabrication process has been performed with the optimized parameter with the constant feed and the constant voltage shows in Table 3.1. And Fig 3.1 shows WAAM schematic setup, and Fig 3.2 (a-b) manufactured sample and Fig 3.2 (c-d) after cut through wire EDM, in this process with the help of 0.8 mm NiTi wire was deposited over the titanium substrate through metal inert gas welding.

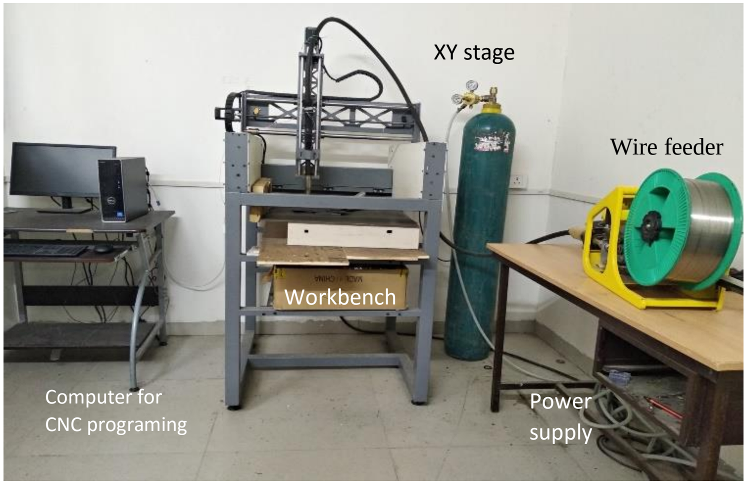

Fig 3.1 Actual photograph of WAAM setup

After fabrication, a bulk structure sample was prepared using CNC wire (Electron Discharge Machining) EDM ecocut model with a resolution of 0.001mm to cut the workpiece from bulk structure to the required dimension. The sample size of 50x1x1 mm this strip was used for laser diffusion and laser annealing.

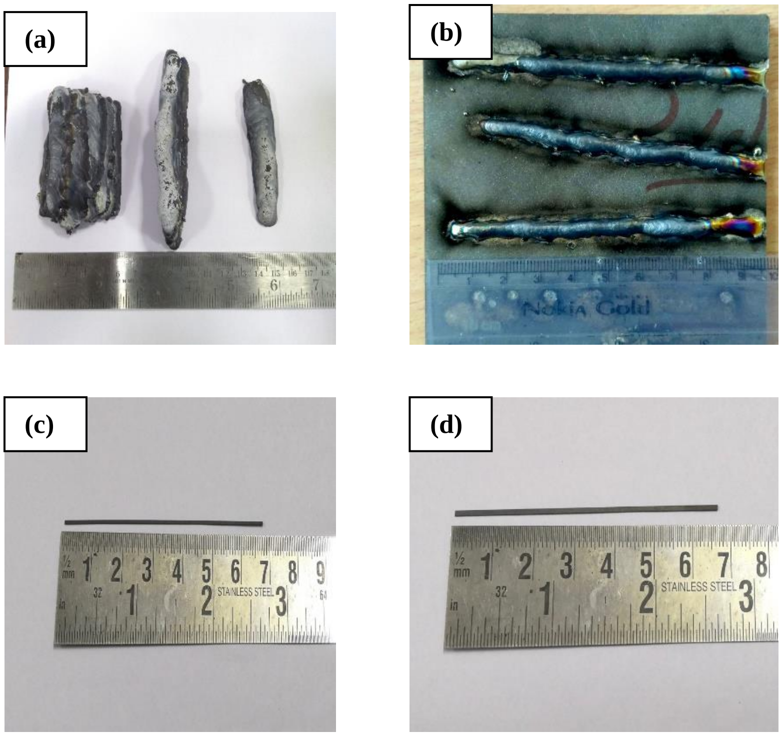

Fig 3.2 (a-b) WAAM fabricated sample, and (c-d) after cut through the wire-EDM

3.5 Results and discussions

3.5.1 Morphological analysis

The grain boundaries of the WAAM fabricated NiTi that grain could be visible with needle-shaped martensite contained by the grains. The change in grain size has been noticed across the various sections of the deposited layer as shown in Fig 3.3. This difference in grain size could be attributed to temperature gradient existed during deposition across the depth. The bottom might have higher cooling rate due to the substrate.

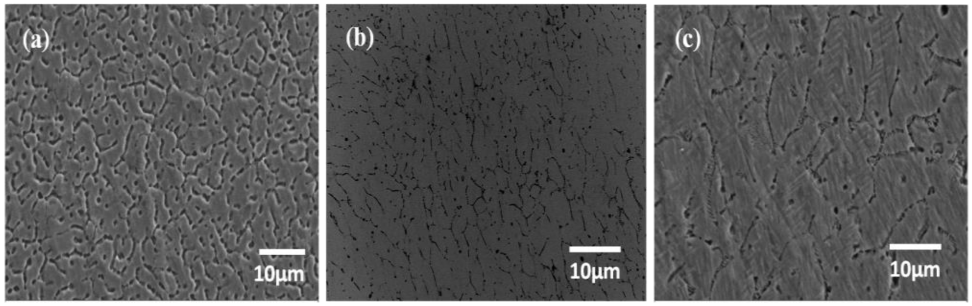

Fig 3.3 FE-SEM images of (a) bottom section, (b) cross-section and (c) top section of AM NiTi

3.5.2 Structural analysis

Phases present were identified based on peaks from the JCPDS card for the B2 phase and 03-065-3957 for rhombohedral R-phase. The XRD spectrum of as-fabricated NiTi Fig 3.4 consist of the main peak at 42.48˚ (110) which corresponds to B2 cubic austenitic phase along with other cubic lattices at 440, 200 and 211 reflections. As-fabricated XRD pattern also shows traces of (R-phase) at 25.32˚ (021).

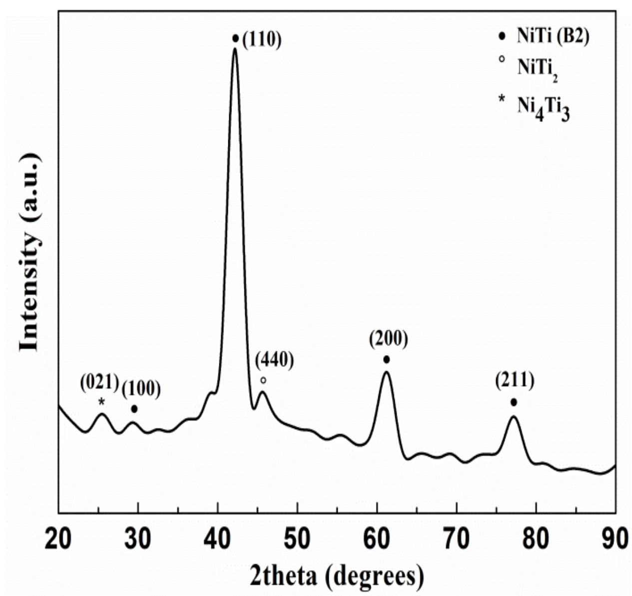

Fig 3.4 XRD patterns of fabricated NiTi

3.5.3 Microhardness analysis

The micro-hardness analysis of the NiTi deposited sample showed that the value varied between 300 HV to 400 HV as shown in Fig.3.5. The bottom section had the comparatively higher hardness value and the top section the lowest. The measured average values at the bottom section, cross-section and top section are 385.67 HV, 351.3 HV and 335.67 HV respectively.

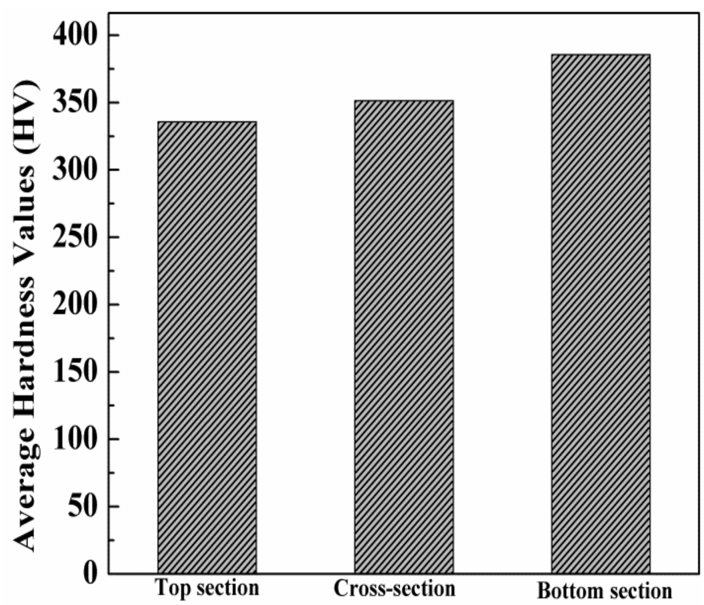

Fig 3.5 Average hardness profile along 3 different sections of AM NiTi

3.5.4 DSC analysis

The thermal analysis was carried out on the NiTi sample and specimen in order to report the changes in phase transformation characteristics. The transformation temperatures are expressed as A_s, A_f, M_s, M_f, R_s and R_f (austenite, martensite and R-phase starting and finishing temperatures respectively). A_p, M_p and R_p mean the peak temperatures for the concrete transformations. In the DSC graph of NiTi sample as shown in Fig 3.6. we can notice shallow austenite and martensite peaks.

Table 3.2: Transformation Temperatures (°C) of WAAM fabricated NiTi

Sample	A_p	A_s	A_f	M_p	M_s	M_f	R_p	R_s	R_f
NiTi	9.76	-17.12	27.36	2.56	22.72	-19.2	-	-	-

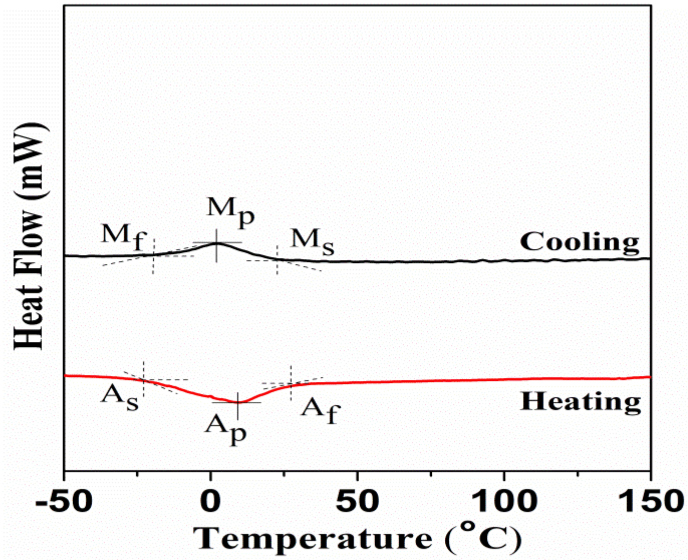

Fig.3.6 DSC plot for NiTi sample

3.6 Summary

In this chapter, the bulk structure of the SMA has been successfully fabricated using Wire Arc additive Manufacturing (WAAM) technique. AM is a technology that makes a promise to reduce product cost and material time. And, the independent of the part feature, AM does not require the blank and it is the full automation and fast process, complex work is done easily. After the fabrication part, we have done characterization such as structural analysis, microhardness, and phase transformation. NiTi deposited sample showed the microhardness value from 300 HV to 400 HV. The change in grain size has been noticed across the various sections of the deposited layer.

Chapter 4

Investigation on Laser Diffusion of copper in the WAAM fabricated SMA Structure

4.1 Diffusion

Diffusion is basically mass transfer. It would happen in solid, liquid and gas. This diffusion, main interest towards the solid. In this work, we have done the laser diffusion by using Solid state nanosecond Nd: YAG pulse laser. After fabrication through the AM and then copper was deposited over the WAAM fabricated NiTi sample by using DC magnetron sputtering deposition technique then laser diffusion performed on copper coated NiTi sample.

4.2 DC magnetron sputtering

DC magnetron sputtering is work on the principle of the momentum transfer when the power was supplied to the magnetron gun then start blowing the gun. Negative electro potential applies to magnetron and ground references of the chamber is positive. Chamber has filled the process gas argon then free electron accelerates away from the gun when these electrons collide with argon gas atom they stick the gas atom and created a positively charge ion as shown in Fig 4.1. These positive charge particles accelerate towards the magnetron, these ions have enough energy to knock off some of the magnetron charge species. These changes material within collect with the surface of the substrate and passes where the direction of the magnetron. Positively charge particle recombine with the free electron to create neutral atomic ions. From the gun light plasma recreated and recombine with free electron into a lower state, it had a voltage and Electron need less voltage, so these access voltages layered on the light, the light was the plasma glow which seen during the process [15,21]. For that process following parameter is used which was given in Table 4.1, copper target material was used with 99.99% purity.

Table 4.1 Parameter of DC Magnetron sputtering

Target Material	Substrate Material	Target Dia. (mm)	Target Thickness (mm)	Deposition time (min.)	Angle (^{0})	Pressure (mBar)	S.O.D. (mm)	Voltages (V)	Current (A)
Copper (Cu)	WAAM fabricated NiTi sample	50	2	10	50	5×10^{-5}	80	390-483	0.55

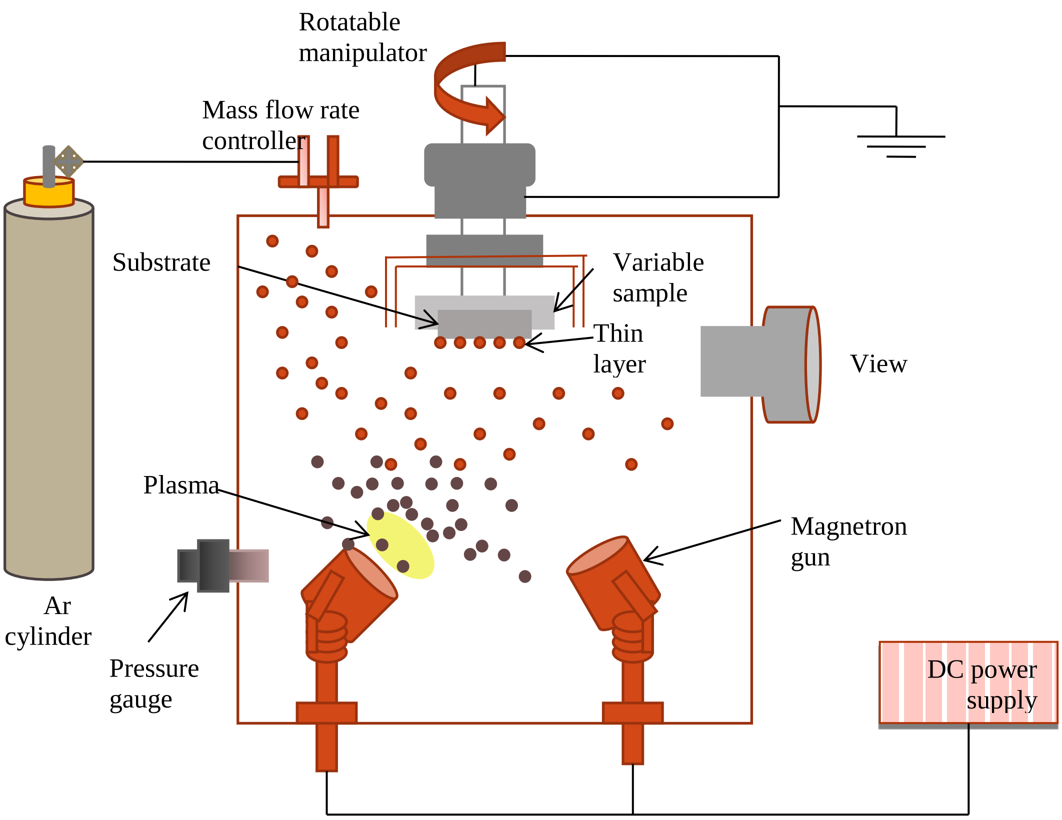

Fig.4.1 Schematic representation of DC magnetron sputtering

4.3 Laser diffusion

The laser diffusion experiment has been performed by using Solid state nanosecond Nd: YAG pulses laser as shown in Fig 4.2. Optimized parameter was used for the laser operation such as wavelength, power, stand of distance (SOD) and spot diameter as given in Table 4.2 laser diffusion has been done on WAAM fabricated copper sputtered NiTi, in this experiment when the 355 nm wavelength of laser beam passes through the lens it would focus on the SMA structure as shown in figure 8. Because of the high concentration of the laser, that laser diffused the coated copper to the NiTi, during the process we have used 90% overlap to the adjacent laser path.

Table 4.2 Parameter for the laser diffusion work

Wavelength (nm)	Power (W)	Spot diameter (μm)	S.O.D (cm)
355	0.5	200	30

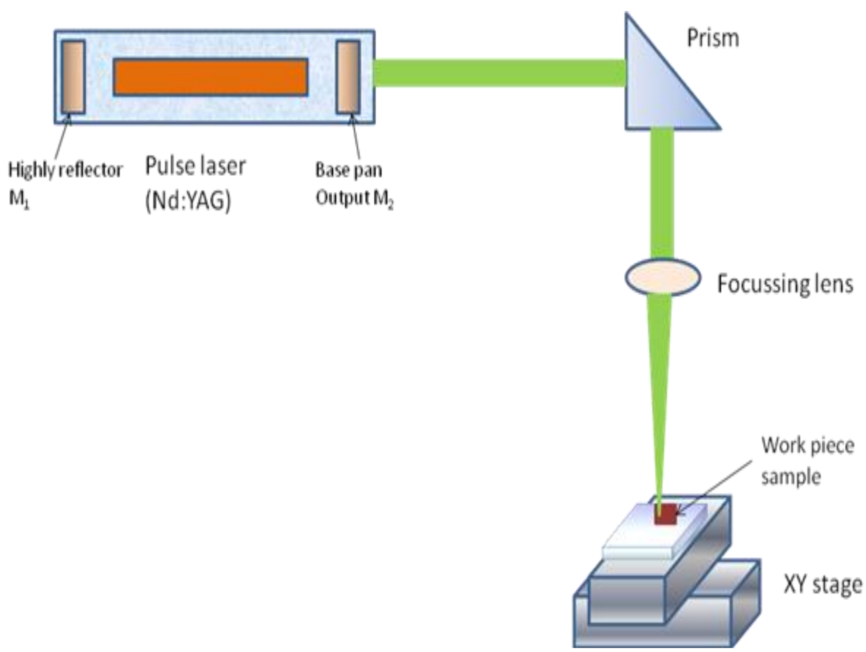

Fig 4.2 Schematic representation of laser diffusion

4.4 Results and discussions

4.4.1 Morphological analysis

The optical microscope images we have taken before or after the laser operation, in this process we have observed that, We have observed that, WAAM fabricated sample found pore and pits that were clearly visible and after the copper was deposited over the fabricated sample then it was plan, but after the laser was treated the upper layer of the copper, then copper was accumulated and diffused over the surface, some pore and crack were found during laser diffusion as shown in Fig.4.3.

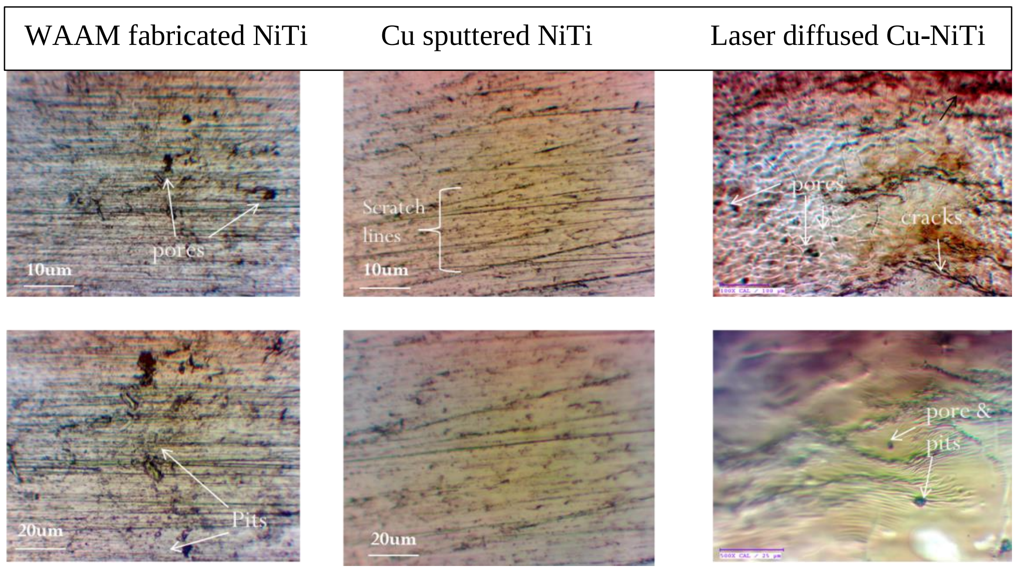

Fig 4.3 Optical microscope images

In the field emission scanning electron microscopy (FESEM) images of WAAM fabricated sample, line scratches of the emery paper during the polishing have been observed. But in the Cu sputtered NiTi sample copper particle has been observed and after the laser diffusion copper is accumulated and diffused over the surface when the laser is focused on the surface as shown in Fig 4.4.

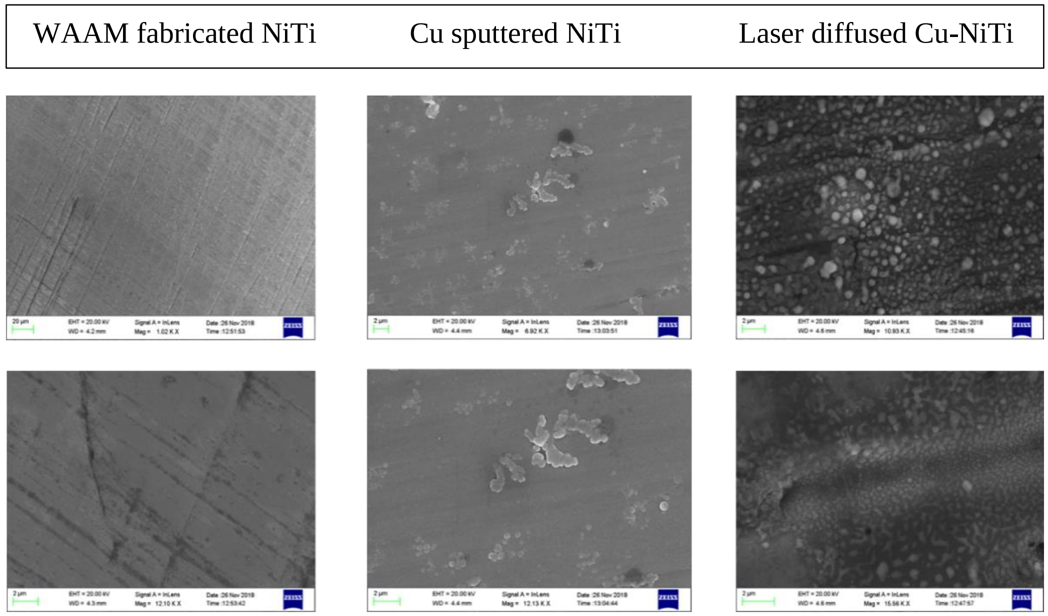

Fig.4.4 FE-SEM images of WAAM, cupper sputtered and Laser diffused Cu-NiTi

4.4.2 Compositional analysis

The energy dispersive x-ray spectroscopy (EDX) images and spectrum revealed the compositional analysis of the WAAM fabricated NiTi sample, copper sputtered NiTi sample and the laser diffused NiTi sample. Nickel and titanium were found in all three samples, but copper and iron were also found in the sputtered and the laser processed sample as shown in the Fig.4.5 and Table 4.3.

Table 4.3 Compositional of the fabricated, sputtered a laser diffused sample

Name Element(wt%)	Ni (wt %)	Ti (wt %)	O (wt %)	Cu (wt %)	Fe (wt %)
WAAM fabricated NiTi	43.06	39.72	15.21	0.63	0.84
copper sputtered NiTi	31.96	27.72	21.53	18.57	0.31
laser diffused NiTi sample	32.52	27.50	13.80	25.80	0.38

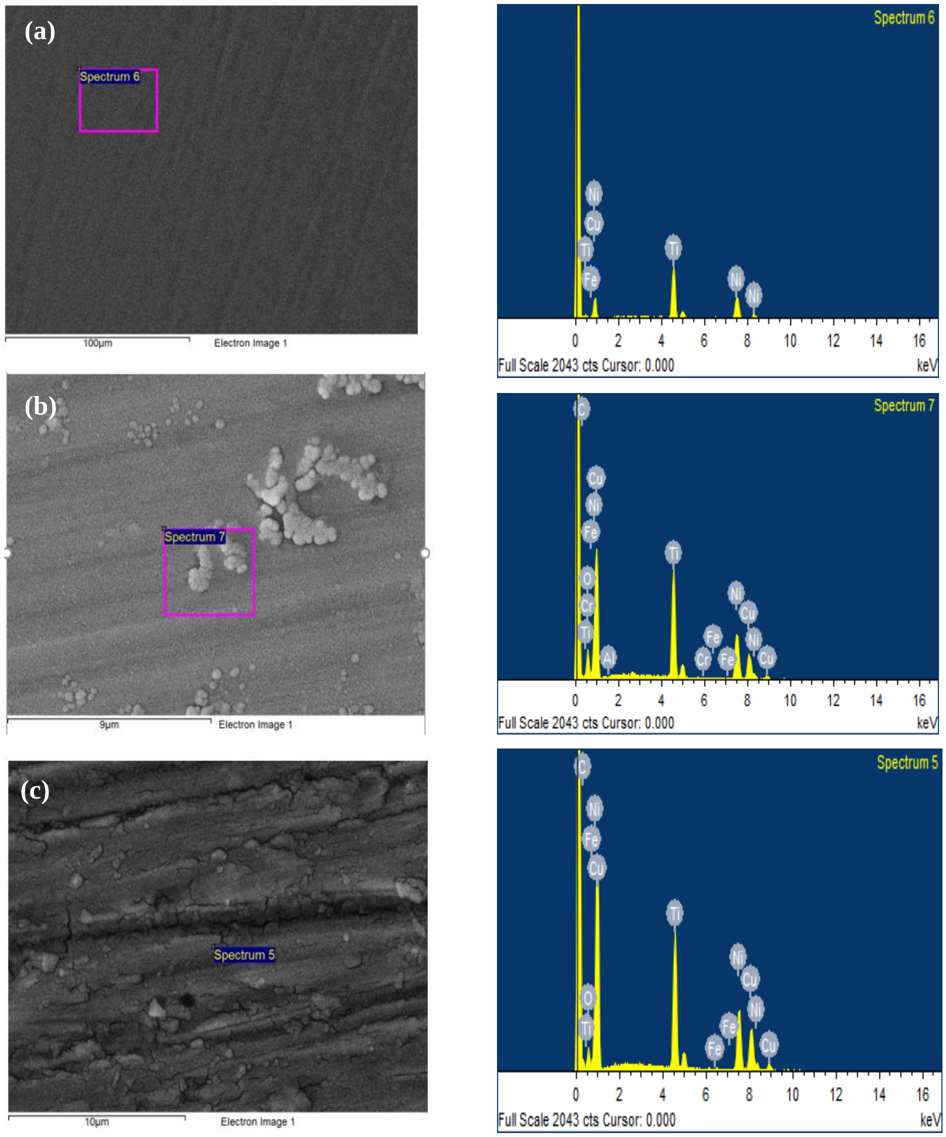

Fig 4.5 Energy Dispersive X-Ray Spectroscopy images (a) WAAM fabricated NiTi sample, (b) Cu sputtered NiTi sample, (c) Laser diffused Cu-NiTi sample

4.4.3 Structural analysis

Phases present were identified based on peaks from JCPDS card number 000440113 and 000561142 for the monoclinic and the tetragonal structure. The XRD spectrum of as-fabricated copper sputtered NiTi and laser diffused NiTi Fig. 4.6 (a)and (b) consist of the main peak at 42.68˚ (020)

and 61.30˚ (003) in both the graph as shown in Fig.4.6, one more peak consist at 36.84˚ (101) with the monoclinic crystal structure.

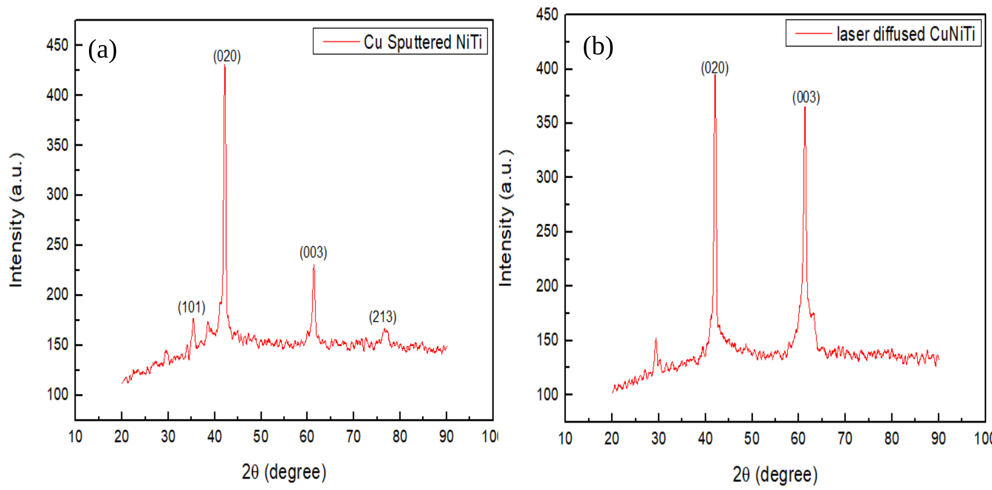

Fig. 4.6 Graph (a) and (b)the X-ray diffraction results

4.5 Summary

After fabricated of the bulk structure using WAAM to be introducing a ternary element, we have to adopt a different manufacturing process for copper deposition over NiTi, known as DC magnetron sputtering. By sputtering a thin layer of copper is deposited over the NiTi sample for making a sample of copper coated nickel-titanium (Cu-NiTi). then with the help of Solid-state nanosecond Nd: YAG pulse laser was diffused over the surface of the copper coated nickel titanium, We have observed that WAAM fabricated sample found pore and pits that were clearly seen and after the copper was sputtered over the fabricated sample then it was plan, the laser was treated the upper layer of the copper, then copper was accumulated and diffused over the surface.

Chapter 5

Investigation of Laser Annealing of WAAM fabricated SMA Structure

5.1 Annealing

Annealing is a process in order to make it better the surfaces of materials while first heating the material and then after cooling the material, methods of heating including these by lamps, laser or furnaces annealing. Laser annealing, as the words focused, performing the annealing that passes the laser beam by lens focus over the surface then after the cooling process, the sample can perform in the air itself. The component of laser basically used for the annealing od sample by the scanner, scanning the surface of a material by using a condensing lens for focusing a laser beam.

5.2 Laser Annealing

The schematic representation an actual photograph of the laser experiment setup is presented in Fig 5.1 Ytterbium-doped fibre Laser is used for the

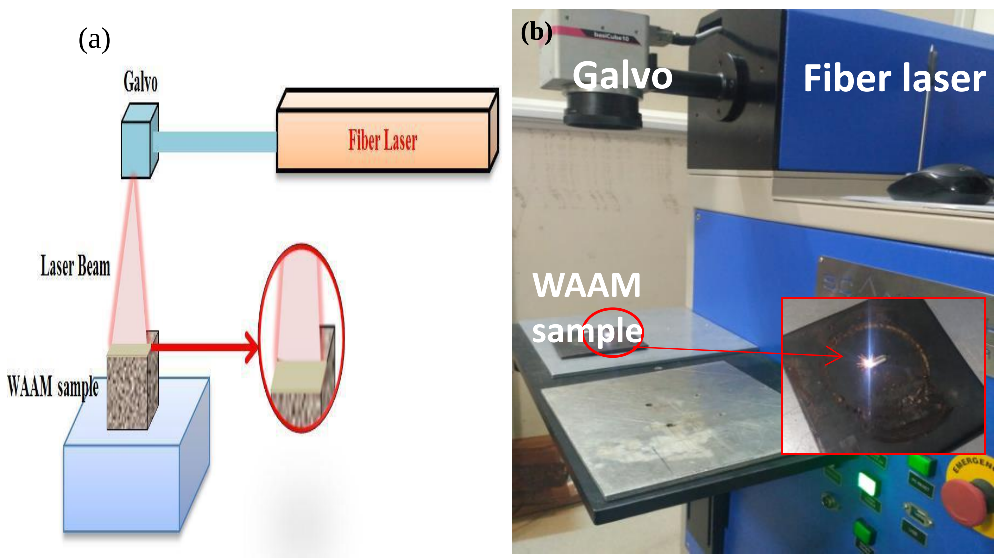

Fig.5.1 (a) Schematic of the Laser Polishing process, (b) Actual photograph of ytterbium-doped fibre Laser

annealing with optimizing parameters such as wavelength 1064 nm, power 50W, number of passes 40, output power 50, pulse width 0, and the marking speed is 20 mm/sec.

During optimization, we plot the graph between Power and temperature, power starting from 10 to 50 watt and the variable temperature value were getting. And kept the output power 50 and number of passes 5 as shown in Fig 5.2.

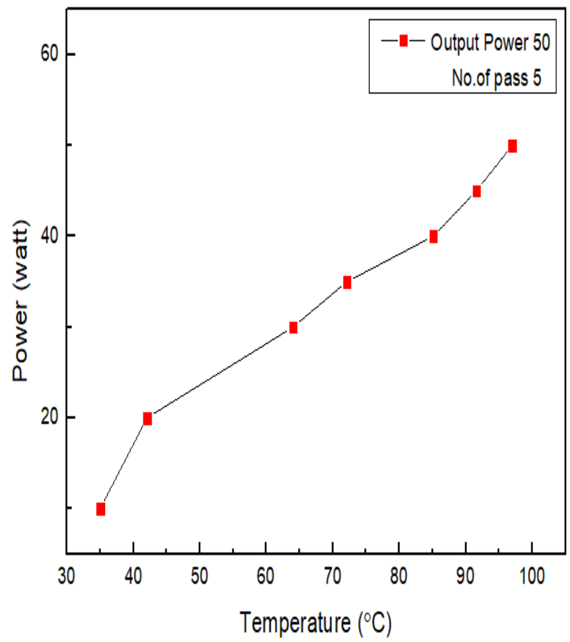

Fig.5.2 Plot between Power-Temperature graph

5.3 Results and discussions

5.3.1 Thermo-Graphic images

The thermo-graphic images of the annealed sample were taken by the FLIR ONE camera with varies the power and the kept the number of passes constant and got the temperature as shown in Fig.4.3 and this images 50 watts and the 5 number of passes get the maximum temperature.

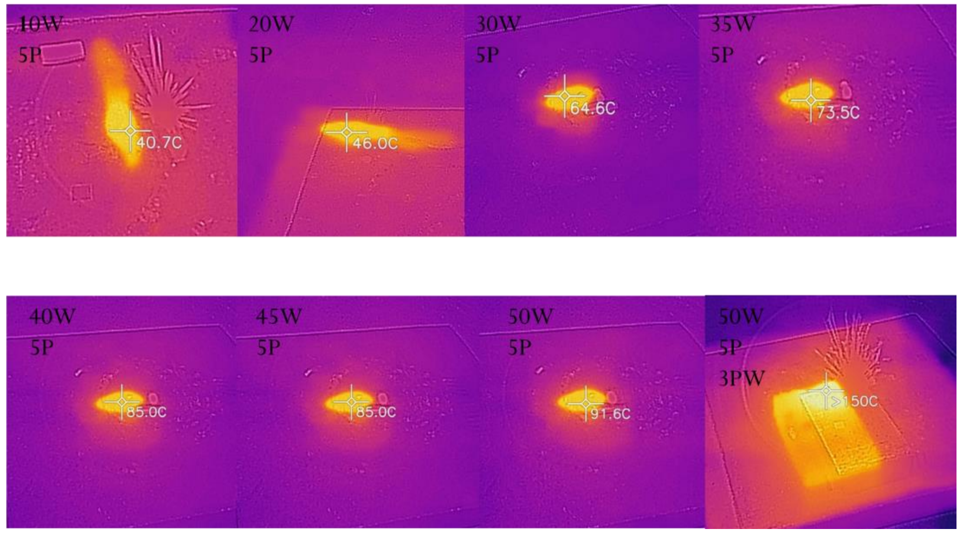

Fig.5.3 thermo-graphic images of the annealed sample

5.3.2 Optical microscopic images

Optical microscopic images have been taken to identify to avoid the re-melting, resulted due to the laser annealing as shown in Fig.5.4 we were used 50-watt power and 40 number of passes with constant pulse width is 0. If we increase the pulse width, then heat affected zone increases and re-melting also happens in order to avoid this we optimize the parameter.

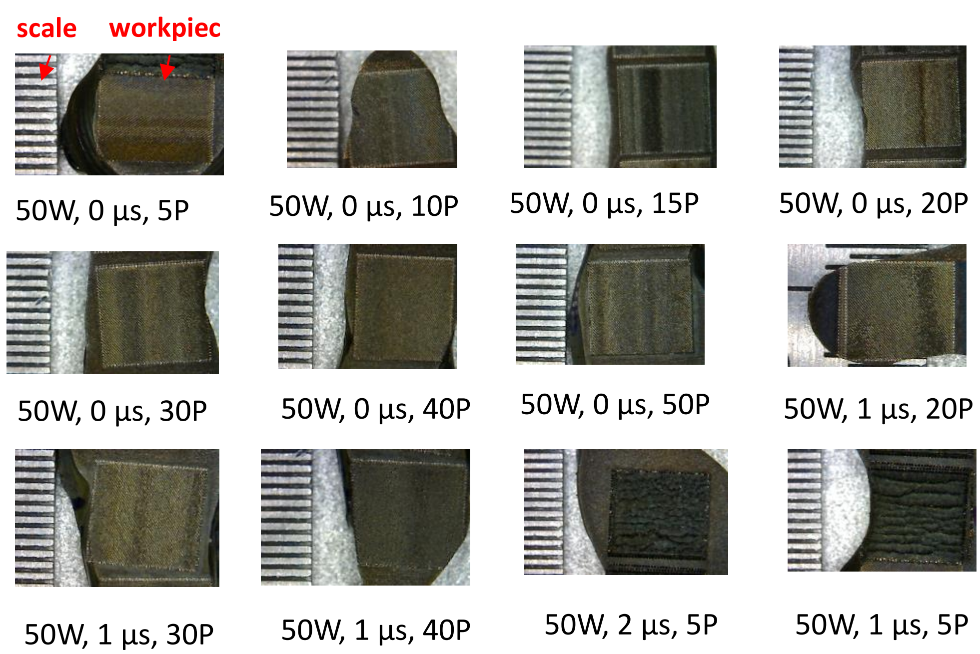

Fig.5.4 the optical microscope images of the sample

5.3.3 Temperature measurement using a thermocouple

During laser annealing, we need to measure the temperature of the sample and the temperature of the laser which are spotted over the fabricated sample and the. For that, we used the thermocouple for measured the temperature along with Data acquisition (DAQ) system is shown in Fig 5.5 (a). Initially, we measured the spot temperature of the laser which is the focus over the sample that was 550°C and the temperature of the sample goes around the 400°C which is shown in Fig 5.5 (b). In this setup, we used 50W power with 10 number of passes for measuring the temperature and after a certain number of passes it gave the constant temperature that's why we used the 10 number of passes.

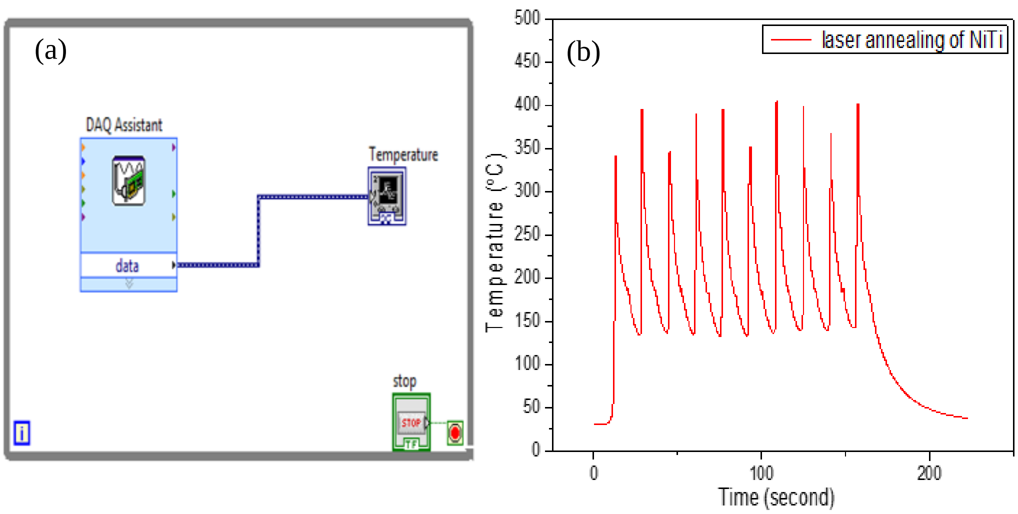

Fig:5.5 (a) schematics experimental setup, and (b) plot between time and temperature

5.3.4 Differential scanning calorimeter analysis

The DSC curve of the WAAM fabricated NiTi sample as shown in Fig 5.6 the austenite start and finish temperature (A_s, A_f) and martensite start and finish (M_s, M_f) transformation temperatures [22]. These transformation temperatures are given as an inset in Fig.8. In this figure, Fig 5.6 (a) shows the DSC curve of the untreated sample and the and Fig 5.6 (b) shows the laser treated sample.

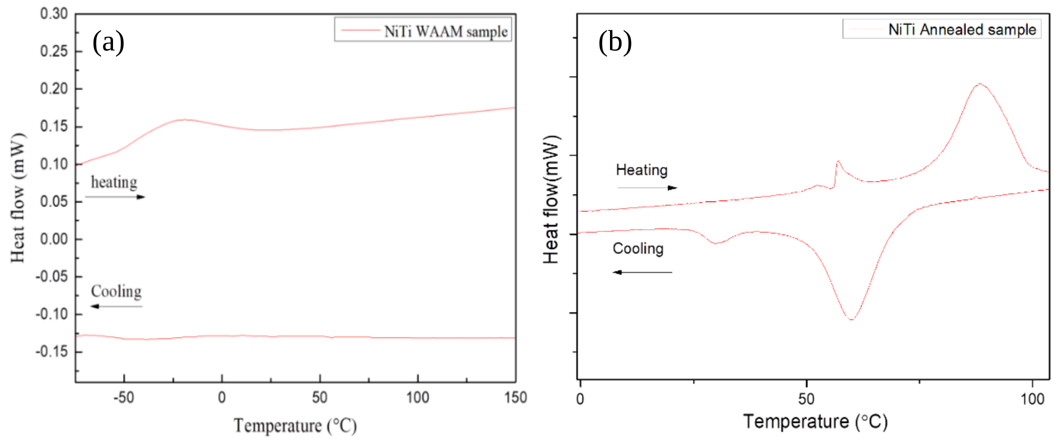

Fig.5.6 (a) DSC plot of NiTi untreated sample (b) DSC graph of the NiTi treated sample

5.3.5 Shape memory effect

Since WAAM fabricated sample was annealed at more than 450°C using ytterbium-doped continuous laser and the sample left for the cooling at room temperature without any disturbance for about to 12 hours then after executed it was completely recovered strain. The actuation of the laser annealed was quantified by recovery angle using hot plate actuation. The duration for complete strain recovery was noted to be 26 s, elsewhere that there was no change after this in the sample it was straight. For a change the annealed sample from deformed martensite into undeformed martensite we gave the applied bending stress by hand. on heating, austenite transformation started then it will convert to its original shape [23,24]. The recovery angle and time plot is shown in Fig 5.7 (g) and the actuation of the photo at room temperature and the austenite temperature during the actuation is shown in Fig.5.7 (a - f).

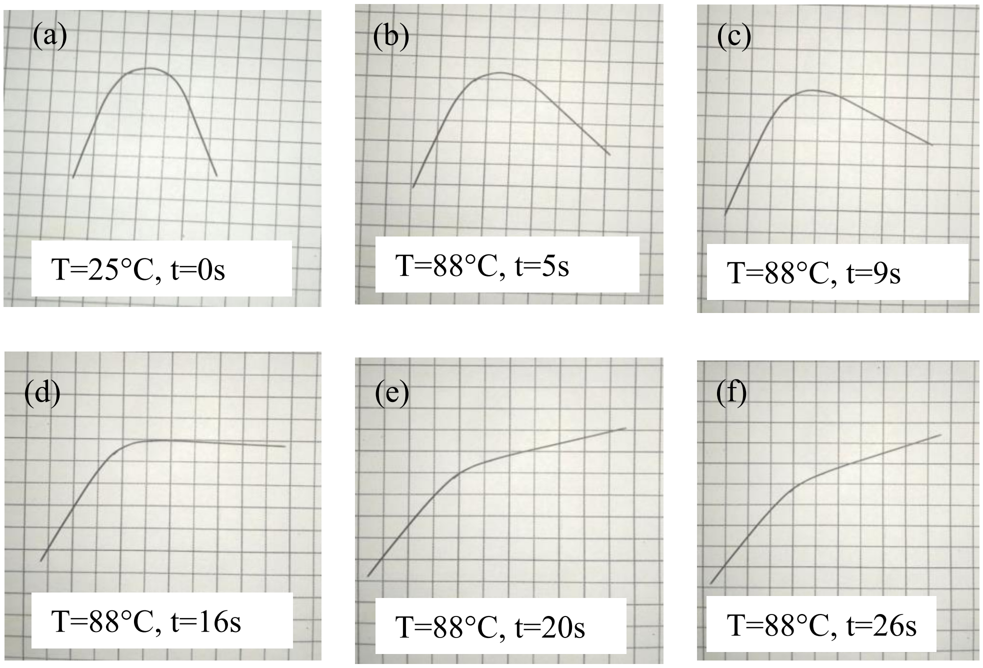

Fig:5.7 the hot plate actuation of the NiTi annealed sample with (a) room temperature and (b - f) is austenitic temperature during actuation.

The graph between the recovery angle and the time which is shown in Fig.5.8 (g). after the annealing hot plate actuation has been performed with the austenite set temperature 88°C. the temperature reached to set temperature after that we put the detwinned martensite sample over the hot plate then start austenite transformation [25]. Duration transformation we have captured the snapshot of the sample with the different-different time up to full recovery.

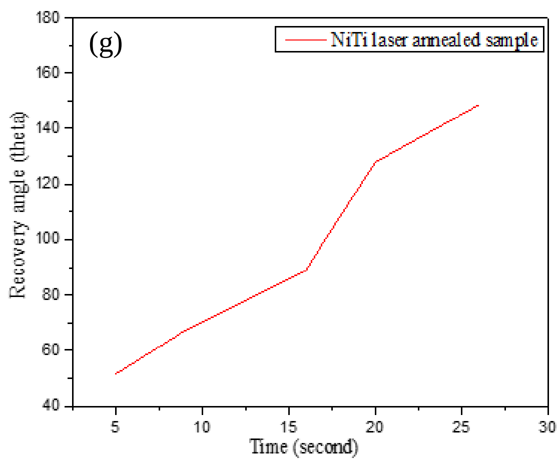

Fig:5.8 (g) plot between time and the recovery angle

5.3.6 UTM measurement

A tensile test is measurement has been performed for determining the characteristics of the material under tensile loading as shown in Fig 5.9. The test was conducted by fixing the work sample into the testing device and the applying force to the sample. UTM machine has the capacity of 2kN, and the Maximum Force (F_m) is 225.800 N, Displacement at F_m is 0.980 mm and maximum displacement is 1.159 mm.

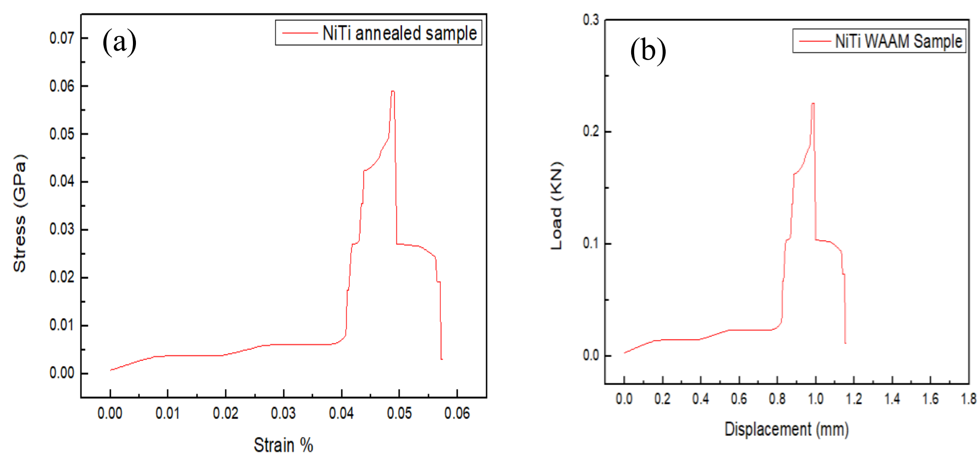

Fig.5.9 (a)Stress-strain graph (b) load-displacement graph

5.3.7 Structural analysis

The crystallographic change on the NiTi due to the laser annealing was studied using X-ray diffraction analysis. Fig.8.10 The sharp peak at 42.99° was describing an austenite phase of the lattice (110), and at 76.55° (220) in Fig 8.10(a). And the Fig 8.10(b) the sharp peak at 44.27° was describing the lattice (23-1) and at 41.38° the martensite phase of the lattice (111).

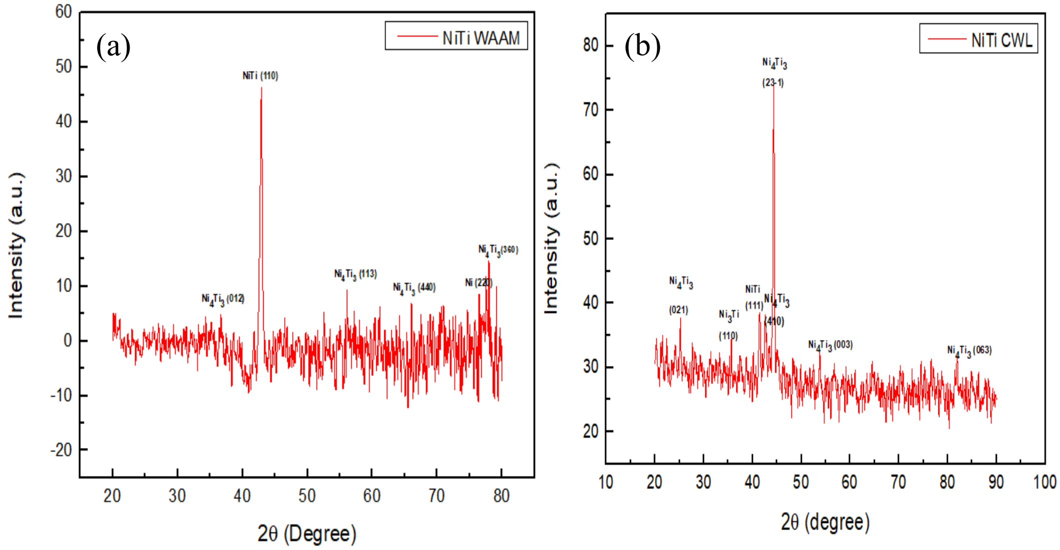

Fig.5.10 (a) XRD graph of the NiTi WAAM sample (b) XRD graph of the NiTi CWL sample

5.3.8 Surface Morphological Analysis

In this the morphology of the upper surface of the sample that we have taken by using the Dewinter (Dmi prime) optical microscope of upper surface of the NiTi sample as shown in Fig 5.11 from figure (a) to (c) shows the optical microscope images of the before laser annealing and Fig (d) to (f) shows the after-laser annealing. The morphological analysis of the top surface of the with or without laser annealing, it can be observed that final grain size for the 550°C annealing temperature as the time at that temperature increases then the grain size is also increasing. Apart from that yield and tensile strength is decrease and the ductility is increased.

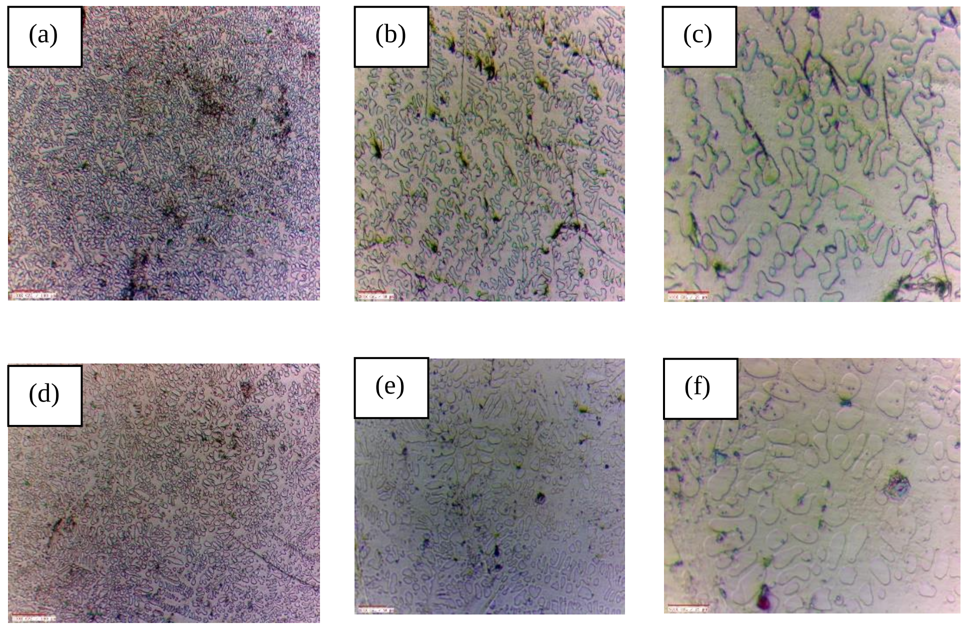

Fig.5.11 Optical microscope images (a-c) before laser annealing (d-f) after laser annealing

5.4 Summary

In this chapter, we have done laser annealing using ytterbium-doped continuous fibre laser over a thin strip of 8×1×0.5 mm thickness SMA. Parameter of the laser process was 1064 nm wavelength, 50 W power and 40 number of passes. Temperature measurement by thermocouple with 50W power and 40 number of passes for getting the temperature around 400°C-450°C. The actuation of the laser annealed was quantified by recovery angle using hot plate actuation that shows the SME.

Chapter 6

Investigations on Laser assisted shock peening of the untwined NiTi SMA structures

6.1 Laser Shock Peening (LSP)

Laser shock peening (LSP) is one of the utmost advanced surface enhancement technique which has been widely used in the automobile industry, steel industry and medical implants [24]. LSP is a surface and tribology engineering process used to convey important residual stresses in materials. The deep, higher compressive residual stresses succeed by laser peening to enhance the resistance to the surface of materials kinds of failures, such as fatigue, wear and tear, fretting fatigue and stress corrosion and cracking [25]. The physics of the LSP process can be used to stronger thin sections, treated surface, shape or stronger parts called as laser peening, break up hard materials, dense powdered metals and for shock waves, short duration and high-pressure application.

In a Q-switched mode, the population inversion is achieved permissible to accumulation by appearing the loss inside the resonator that surpasses the increase of the medium, this can also be described as the decreasing the factor of quality of the cavity. When the drive energy kept in the laser medium has closer to the extreme feasible side, the experienced the loss mechanism is suddenly removed, allowing of substance to start which suddenly gain the deposited energy in the increasing medium.

In this work, laser shock peening of the NiTi shape memory alloy by Q-switched mode Nd: YAG pulse laser source of the wavelength of 1064 nm with 90% overlap to adjacent spot has been carried out. Further, analysis of the effect of laser deformation on the surface has been done to analyze the phase, grain size and the microstructure [26].

6.2 Experimental setup

The sample for LSP was prepared using CNC wire (Electron discharge machining) EDM ecocut model with a resolution of 0.001mm to cut the workpiece from raw material. The sample size of 15 × 15 mm was used for LSP. After cutting the sample, mechanical polishing using SiC papers of grit size 120 to 2000 has been carried out to remove the oxide film and to get an even surface and we achieve external roughness after polishing is 1.93 µm from 11.34 µm using Vicco Optical profilometer as shown in Fig 6.1. shows the images of the sample before and after polishing.

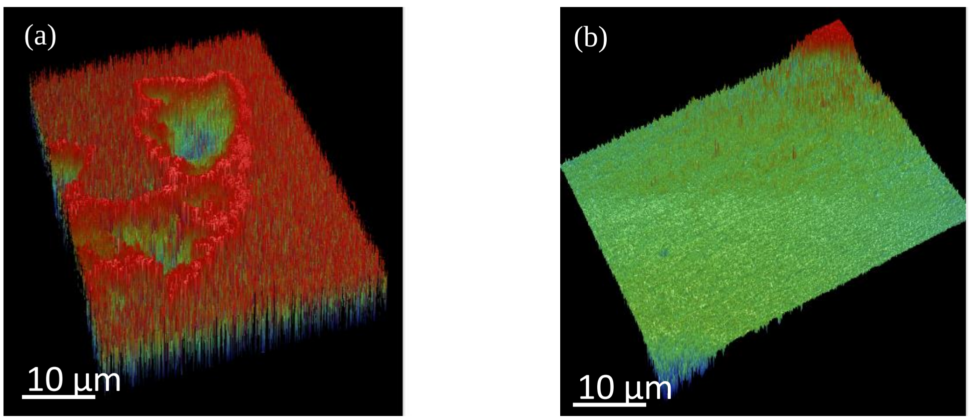

Fig 6.1 Vicco Optical profilometer (a) Before polishing, (b) After polishing

6.3 Laser Peening

The schematic of laser representation of experiment setup is shown in figure 2. Laser from a source of Q-switched mode Nd: YAG pulse laser working with a wavelength of 1064 nm, with one pulse for every 10 ns was used to peen the target material placed at 30 cm focal length.

An XY moving stage was also arranged by connecting the servo motor. The pulse density of the LSP process was measured by the speed of the translation stage. The beam diameter of the laser was controlled by altering the place among sample and focusing lens. There were no protective layers on the sample to shield the sample surface from heating outcome during the

LSP. And LPS parameters used in the present work is discussed in Table 6.1. And we have used a thin protective layer of water for minimized the transmission loss by presenting a thin water layer over the top of the target surface in its place of immersing the sample under water [26].

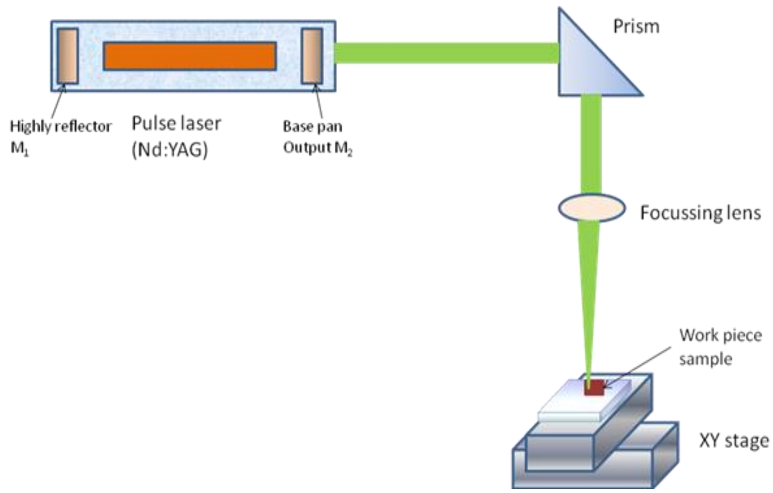

Fig 6.2 Schematic representation of laser shock peening

Table 6.1: Experimental parameters

Sample	Wavelength (nm)	Power (w)	Focal length (cm)	Pulse (ns)	Spot diameter (µm)	Fluence (J/mm^2)
1	1064	1	30	10	200	3.8130

6.3 Results and Discussion

6.3.1 Optical Microscopic Images

Optical microscopic images have been taken to recognize the deformation outcomes because of the LSP. After solidification, the particle size and surface of the NiTi sample has been changed and deformation of the upper layer was observed [26].

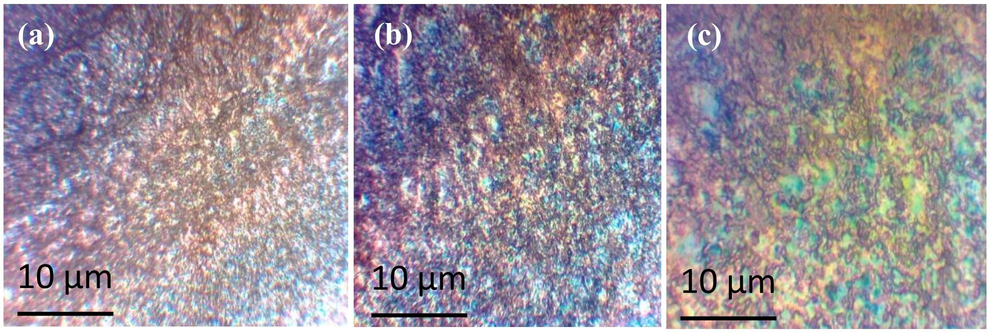

Fig 6.3 Optical microscopic images of NiTi laser shock peened samples (a) 100x, (b) 200x, and (c) 500x

6.3.2 Structural analysis

The crystallographic change on the NiTi due to the LSP was studied using XRD analysis as shown in Fig 6.4 (a) (b) shows diffraction graphs of NiTi sample before and after peening. Due to the LSP, at (002) a monoclinic martensite phase was observed and the remaining peak was cubic austenite phase [27,28].

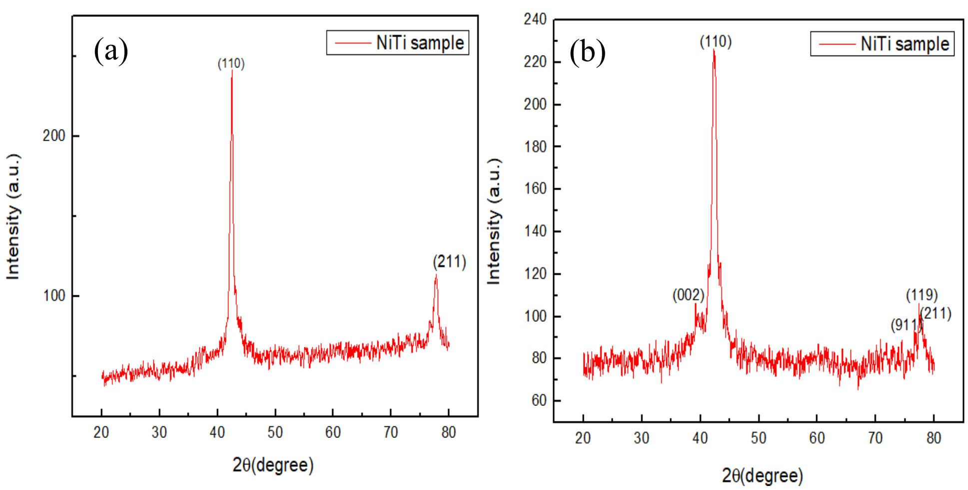

Fig 6.4 XRD graph of the NiTi sample (a) before shock peening, (b) aftershock peening

6.3.3 Microhardness test

Microhardness test is performed on NiTi sample before and after LSP. The microhardness value of unpeened surface is observed as 327 HV, however, aftershock peening near peened surface microhardness value is enhanced to 339 HV [26].

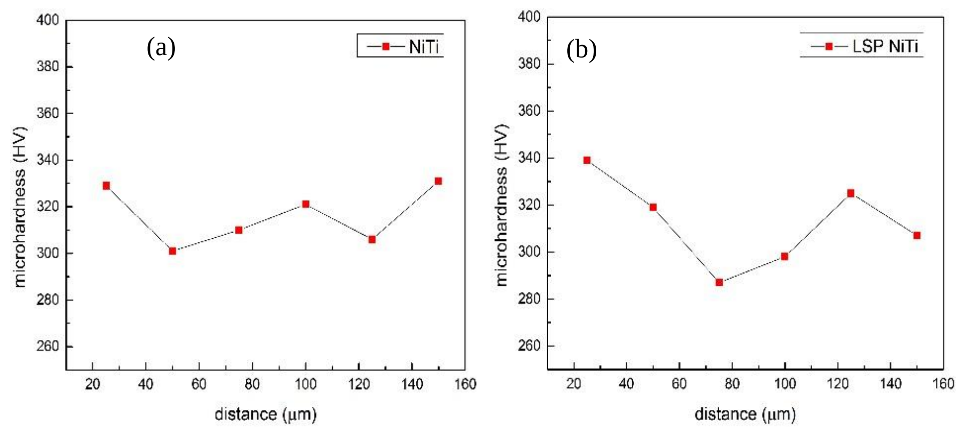

Fig 6.5 Microhardness test measurement graph, (a) before LSP (b) after LSP

6.4 Summary

This section discusses the investigation on laser shock peening (LSP) of the untwined NiTi shape memory alloy structure. The sample was shock peened using solid-state nanosecond Q-switched mode Nd:YAG pulses laser source with the wavelength of 1064 nm with 90% overlap to an adjacent spot. The LSP sample was further investigated before and after laser shock peening by x-ray diffraction, microhardness and optical microscope. After LSP the particle size and surface of the NiTi sample has been changed and deformation of the upper surface was observed, and hardness of the peened surface also increased.

Chapter 7

Laser polishing of Wire Arc Additive Manufactured SS 316L

7.1 Background

A wire arc additive manufacturing method is assisted to the fabrication of thin wall structure with high rate deposition, but this process also requires post-processing such as surface polishing and heat treatment for enhancing the properties [29]. Surface polishing is an important process for removing a thin layer of unwanted materials such as micro, macro and nano size, which is reducing the peak and valleys of the surface [30]. This surface roughness is an important role to influence the mechanical or surface tribology properties, but the conventional polishing process consumes more time of production. So, there is various modern or unconventional polishing processes are suitable for attaining excellent surface finish [31], such as abrasive blasting, mechanical polishing, electrochemical polishing, and laser polishing. Among all these techniques, laser polishing is a potential method to obtain a superior surface finish with low roughness due to the surface melting of the substrate without any modifications in bulk properties [32].

In this research, an austenitic stainless steel 316L is used to fabricate the structures by using the WAAM method in which samples are assisted through laser polishing to attain superior surface roughness. The surface roughness will be evaluated through an optical profilometer and crystalline structure, the impurity content is evaluated by using XRD. The mechanical property of the sample was observed by a microhardness instrument.

7.2 Material and methods

Material

WAAM fabricated, an austenitic stainless steel 316L samples were used for laser polishing process which material chemical composition is shown in table 7.1. This material has exclusive properties such as good strength with high temperature, high corrosion resistance which leads to food production and architectural applications [33].

Table 7.1 Chemical Composition [33]

Grade		**C**	**Mn**	**Ni**	**Mo**	**N**	**Si**	**P**	**S**	**Cr**
316L	Min	-	10.0	2.00	-	-	-	-	-	16.0
	Max	0.03	14.0	3.00	0.10	2.0	0.75	0.045	0.03	18.0

Methods

Wire Arc Additive Manufacturing process also termed as additive manufacturing was performed using ESAB WAAM fabrication system by layer by layer deposition to obtain the desired part. The parts were constructed with an inert gas environment to attain defect-free parts, which parameter is shown in Table 7.2.

Table 7.2 WAAM Parameter

Parameter	Wire feed rate (m/min)	Ar Gas flow rate (l/min)	Voltage (V)	Current (A)	Wire diameter (mm)
Quantity rate	6	20	20	120	1.2

7.3 Laser Polishing

The laser material interaction principles were followed for laser polishing process. SCANTECH fibre laser source was assisted to polish the WAAM fabricated samples with continuous wave laser interaction on the material at a constant wavelength and various powers with no. of the pass which schematic diagram is shown in Fig 7.1. The samples were mounted on the bed with a standoff distance at 30 cm with the wavelength of 1064 nm. Initially, started with low laser power and a number of passes further for governing the parameters, simultaneously increased the power as well as no of passes. The laser polishing process parameter was illustrating in Table 7.3.

Table 7.3. Laser polishing parameters

Sample	Wavelength (nm)	Power (W)	No of pass	Marking Speed (mm/sec)
1	1064	10	5	20
2	1064	10	10	20
3	1064	25	15	20

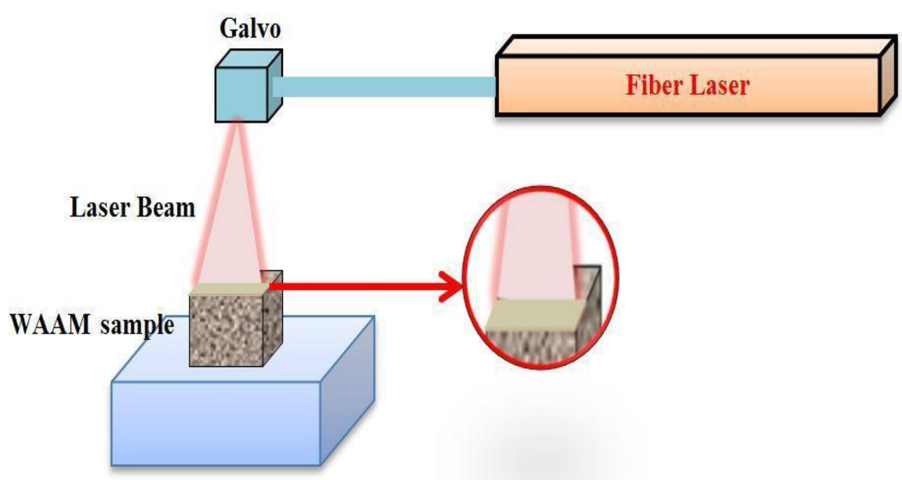

Fig 7.1. Schematic of the Laser Polishing process

7.4 Results and Discussion

7.4.1 Structural Analysis

Rigaku XRD was inured ascertaining the crystal phase changes and structures. The laser polishing process was aided to attain excellent surface finishing for WAAM prepared samples. Two different laser parameters and 3 levels were considered for LP, for which XRD graphs are shown in Fig.2. The sharp peak at 45° was describing an austenite phase of the lattice (111) in sample-1, also with the same sample at an angle of 35.8° and 51.2° peaks confirming that the ferrite structure with different crystal lattices such as Fe_3 (111) and Fe_3 (110). The higher laser power influenced sample-2 shows no sharp peak so, it has confirmed the amorphous structure. Sample-3 has used the lower number of laser scanning passes in which XRD peaks were shifted from 75° to 63.8° respectively as compared with sample-1. In this sample, all the sharp peaks were representing the Austenite phase only but with different crystal lattice at (200) and (220).

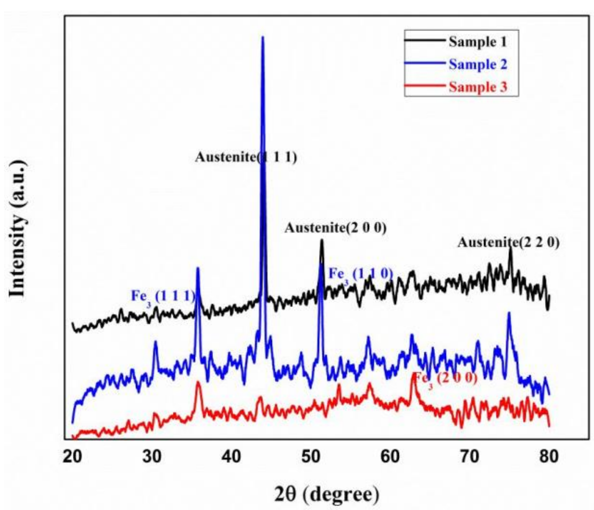

Fig 7. 2 Different laser parameters influenced samples XRD graph

7.4.2 Roughness Measurement

An unconventional evaporation process is required to remove unwanted layers and micro or nanoscale for attaining excellence surface finish. So, Laser polishing was assisted in removing a thin layer from the sample due to laser material interaction principles. Hence it has attained a rough surface. The roughness of the samples was performed with Vecco optical profilometer as shown in Fig 7.3. The average roughness was taken at three different places before and after laser polishing and the values are shown in the table below. There was a 40% reduction in roughness value as shown in Table 7.4 after doing the laser polishing.

Table 7.4 Roughness measurement value

Sample	Pre-polishing Ra value (μm)	Post –polishing Ra value (μm)
S1	14.28	8.45
S2	14.80	9.01
S3	13.50	9.25

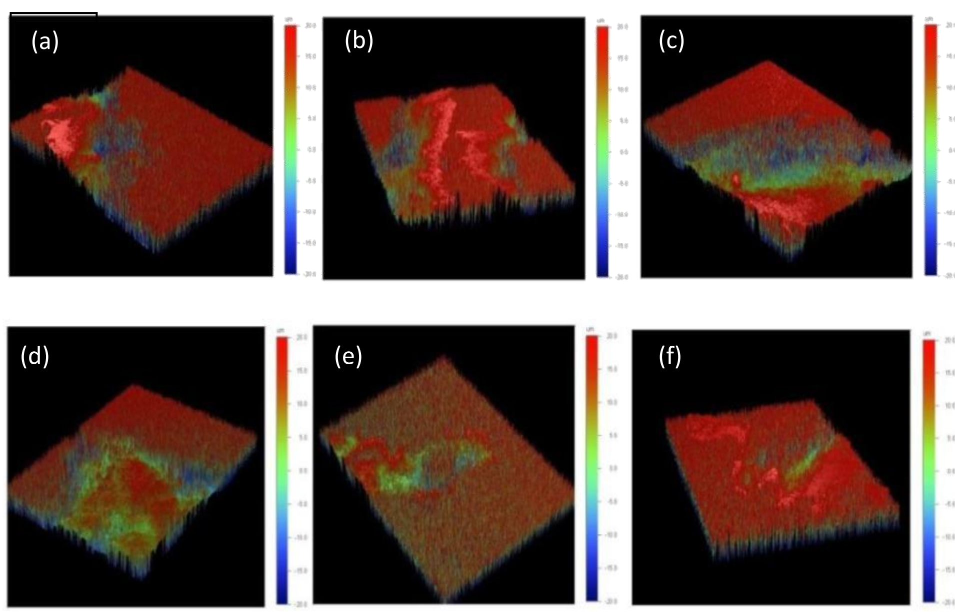

Fig 7.3 Surface roughness images of (a-c) before laser polishing**,** (d-f) after laser polishing

7.4.3 Surface Hardness

UHL Vickers Micro Hardness Testing was used to measuring the microhardness of Laser polished samples. In hardness measurement, the micro indenter load was maintained 200g and a dwell time of 15s also the crosshead speed of 0.025mm/min. To reduce the measurement errors, the polished samples were used to measure in the same cross section to attain the average value. LP sample microhardness profile was measured from top to bottom cross-section with a distance of 0.5mm. The microhardness was gradually reduced from top polished to bottom of the sample1 and 2 at 198 to 178 but sample 3 has high microhardness value (235, 232HV) at the distance of 0.5mm and 4.5mm as compared with other samples which are illustrated Fig7.4. During laser polishing the Laser material interaction, the principle has assisted to remove a thin layer from the surface which ablation has refining the surface grain structures and sizes. Hence, high laser power influenced sample has achieved greater hardness rate as compared to other samples.

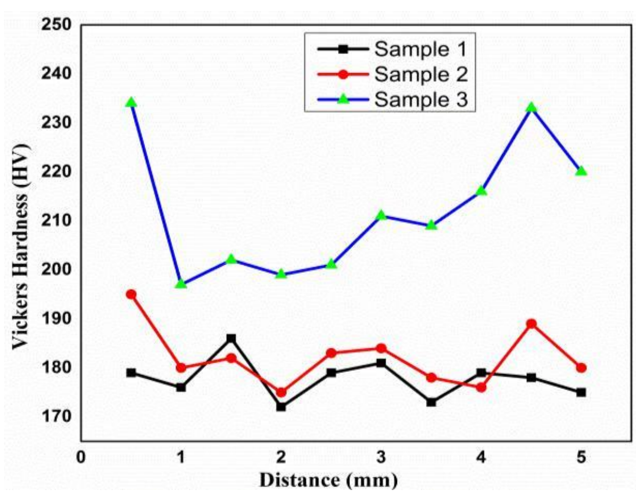

Fig 7.4 Vickers microhardness measurement of laser polished samples

7.5 Summary

Wire-based additive manufacturing has attracted much attention as an encouraging 3D printing technique for metallic material and component as a consumable material in recent year. That seems to contradict that, the surface roughness of the additive manufactured structure and sample has been considered as a challenge to achieve high performance. This paper elucidates the surface analysis of Laser Polished SS 316L samples fabricated using WAAM. The fabricated WAAM samples were polished using Nd: YAG laser source of wavelength 1064 nm at different power and the various number of passes such viz. 10W, 10W, 25W and 8, 10, 15 respectively. The roughness measurement was performed on before and after laser polishing by an optical profilometer and found that 40% of roughness was reduced after laser polishing. The crystal phase changes and hardness were also carried out and validated using XRD and hardness of the laser polished samples.

Chapter 8

Conclusion and Bibliography

Conclusion

NiTi bulk SMA structures by using WAAM with binary and ternary alloy in different compositions were developed. Distinct methodology and technique were used for the fabrication of the work sample, different characterization technique was used for the study of the structural analysis, morphological analysis, compositional analysis, microhardness analysis, phase transformation analysis for this work. Using DC magnetron sputtering Copper was deposited over WAAM fabricated bulk NiTi structure, characterized the work sample after laser diffusion by Solid-state nanosecond Nd:YAG laser over the same copper sputtered NiTi. Laser annealing of WAAM fabricated bulk NiTi structure using Ytterbium-doped fibre Laser for a thin strip of the bulk structure.

8.1 Additive manufacturing using WAAM

- Defect-free NiTi samples were fabricated using WAAM in an argon environment.
- The change in grain size has been noticed across the various sections of the deposited layer.
- Phases present were identified based on peaks for the B2 phase and rhombohedral R-phase.
- NiTi deposited sample showed the microhardness value from 300 HV to 400 HV

8.2 Laser diffusion of copper sputtered NiTi

The laser diffusion experiment has been performed by using Solid state nanosecond Nd: YAG pulse laser and we conclude the following points.

- We have observed that WAAM fabricated sample found pore and pits that were clearly visible and after the copper was deposited over the fabricated sample then it was a plan, but after the laser was treated the upper layer of the copper, then copper was accumulated and diffused over the surface.
- In EDX, Nickel and titanium were found in all three samples, but copper and iron were also found in the sputtered and the laser treated sample.
- In XRD, Phases present were identified based on peaks from JCPDS card number 000440113 and 000561142 for the monoclinic and the tetragonal structure.

8.3 Laser annealing of WAAM fabricated bulk NiTi structure

The laser diffusion experiment has been performed by using Ytterbium-doped fibre Laser with wavelength 1064 nm, power 50W and we conclude the following points.

- The thermo-graphic images of the annealed sample were taken by the FLIR ONE camera, 50 watts and the 5 number of passes get the maximum temperature.
- Temperature measurement by thermocouple with 50W power and 40 number of passes for getting the temperature around 400°C-450°C.
- The actuation of the laser annealed was quantified by recovery angle using hot plate actuation that shows the SME
- In a universal testing machine measurement, the Maximum Force (F_m) was found 225.800 N, max. displacement was 1.159 mm and Max. Tensile Strength was 58.979 MPa.
- The crystallographic change was found on NiTi due to the laser annealing

8.4 Investigations on Laser Assisted Shock Peening of the untwined NiTi Shape Memory Alloy structures

- The laser shock peening operation of NiTi alloys material was successfully performed.
- In optical microscopic images, there were changes in the upper surface of the workpiece and grain size.
- In x-ray diffraction analysis, there were structural changes to the monoclinic structure.
- In the microhardness test, there was an increase in microhardness value of the peened surface.

8.5 Laser polishing of Wire Arc Additive Manufactured SS 316L

- Defect-free SS316L samples were fabricated using WAAM with argon environment.
- X-Ray Diffraction confirms the presence of Austenite and Ferrite phase before and after laser polishing.
- Laser polished samples have shown better surface finish as compared with untreated samples from 14.80µm to 9.45µm.
- High laser power has attained the higher microhardness of 235HV than the low laser power.

Bibliography

[1] B.I.T. Sindri, RESEARCH ARTICLE FUTURE OF SHAPE MEMORY ALLOY AND ITS UTILIZATION * Roy , Int. J. Curr. Res. Vol. 8 (2016) 31646–31651.

[2] S. Jiang, J. Yu, L. Hu, Y. Zhang, Investigation on Deformation Mechanisms of NiTi Shape Memory Alloy Tube under Radial Loading, Metals (Basel). 7 (2017) 268. doi:10.3390/met7070268.

[3] H. Geng, J. Li, J. Xiong, X. Lin, Optimisation of interpass temperature and heat input for wire and arc additive manufacturing 5A06 aluminium alloy, Sci. Technol. Weld. Join. 22 (2017) 472–483. doi:10.1080/13621718.2016.1259031.

[4] H. Ma, C. Cho, Feasibility study on a superelastic SMA damper with re-centring capability, Mater. Sci. Eng. A. 473 (2008) 290–296. doi:10.1016/j.msea.2007.04.073.

[5] C.S. Walter Yang, R. DesRoches, R.T. Leon, Design and analysis of braced frames with shape memory alloy and energy-absorbing hybrid devices, Eng. Struct. 32 (2010) 498–507. doi:10.1016/j.engstruct.2009.10.011.

[6] G. Song, N. Ma, H.N. Li, Applications of shape memory alloys in civil structures, Eng. Struct. 28 (2006) 1266–1274. doi:10.1016/j.engstruct.2005.12.010.

[7] Y.L. Han, Q.S. Li, A.Q. Li, A.Y.T. Leung, P.H. Lin, Structural vibration control by shape memory alloy damper, Earthq. Eng. Struct. Dyn. 32 (2003) 483–494. doi:10.1002/eqe.243.

[8] R.T. Leon, R. DesRoches, J. Ocel, G. Hess, <title>Innovative beam column connections using shape memory alloys</title>, 4330 (2001) 227–237. doi:10.1117/12.434122.

[9] L.D.C. D. J. Hartl, Thermomechanical Characterization of Shape Memory Alloy Materials, in: 2008: pp. 53–119.

[10] Dimitris_C_Lagoudas, Shape Memory Alloys Modeling and Engineering Applications, 2007.

[11] S. Hamidreza, J. Corker, M. Fan, Additive manufacturing technology and its implementation in construction as an eco-innovative solution Automation in Construction Additive manufacturing technology and its implementation in construction as an eco-innovative solution, Autom. Constr. 93 (2018) 1–11. doi:10.1016/j.autcon.2018.05.005.

[12] S. Kapil, F. Legesse, P. Kulkarni, P. Joshi, A. Desai, K.P. Karunakaran, Hybrid-layered manufacturing using tungsten inert gas cladding, Prog. Addit. Manuf. 1 (2016) 79–91. doi:10.1007/s40964-016-0005-8.

[13] K.P. Karunakaran, S. Kapil, H. Vithasth, F. Legesse, Additive manufacturing of H13 tooling element with conformal cooling channel using MIG cladding, Int. J. Rapid Manuf. 7 (2018) 1. doi:10.1504/ijrapidm.2018.10010809.

[14] M.-T. Le, Y.-U. Sohn, J.-W. Lim, G.-S. Choi, Effect of Sputtering Power on the Nucleation and Growth of Cu Films Deposited by Magnetron Sputtering, Mater. Trans. 51 (2009) 116–120. doi:10.2320/matertrans.m2009183.

[15] J.H. Boo, M.J. Jung, H.K. Park, K.H. Nam, J.G. Han, High-rate deposition of copper thin films using newly designed high-power magnetron sputtering source, Surf. Coatings Technol. 188–189 (2004) 721–727. doi:10.1016/j.surfcoat.2004.07.005.

[16] Y. Bellouard, Shape memory alloys for microsystems: A review from a material research perspective, Mater. Sci. Eng. A. 481–482 (2008) 582–589. doi:10.1016/j.msea.2007.02.166.

[17] S.S.M. Prabu, R. Mithun, M. Muralidharan, T. Nath, Thermo-mechanical behavior of shape memory alloy spring actuated using novel scanning technique powered by ytterbium doped continuous fi ber laser, (2019).

[18] S.W. Williams, F. Martina, A.C. Addison, J. Ding, G. Pardal, P. Colegrove, Wire + Arc Additive Manufacturing, Mater. Sci. Technol. 32 (2016) 641–647. doi:10.1179/1743284715Y.0000000073.

[19] N. Knezovi, New Technologies, Development and Application, 42 (2019) 0–7. doi:10.1007/978-3-319-90893-9.

[20] Y. Zhai, D.A. Lados, J.L. Lagoy, Additive Manufacturing: Making imagination the major Limitation, Jom. 66 (2014) 808–816. doi:10.1007/s11837-014-0886-2.

[21] K.K. Ho, G.P. Carman, Sputter deposition of NiTi thin film shape memory alloy using a heated target, Thin Solid Films. 370 (2000) 18–29. doi:10.1016/S0040-6090(00)00947-0.

[22] S. Shiva, I.A. Palani, S.K. Mishra, C.P. Paul, L.M. Kukreja, Investigations on the influence of composition in the development of Ni-Ti shape memory alloy using laser based additive manufacturing, Opt. Laser Technol. 69 (2015) 44–51. doi:10.1016/j.optlastec.2014.12.014.

[23] I.A. Palani, Investigation of Morphological and Actuation Analysis of CuAlNi SMA Coated Optical Fiber, (n.d.).

[24] S.S.M. Prabu, H.C. Madhu, C.S. Perugu, K. Akash, R. Mithun, P.A. Kumar, S. V Kailas, M. Anbarasu, I.A. Palani, Shape memory effect , temperature distribution and mechanical properties of friction stir welded nitinol, J. Alloys Compd. 776 (2019) 334–345. doi:10.1016/j.jallcom.2018.10.200.

[25] K. Akash, A.K. Shukla, S.S. Mani Prabu, D.C. Narayane, S. Kanmanisubbu, I.A. Palani, Parametric investigations to enhance the thermomechanical properties of CuAlNi shape memory alloy Bi-morph, J. Alloys Compd. 720 (2017) 264–271. doi:10.1016/j.jallcom.2017.05.255.

[26] S. Sathyajith, S. Kalainathan, S. Swaroop, Optics & Laser Technology Laser peening without coating on aluminum alloy Al-6061-T6 using low energy Nd : YAG laser, Opt. Laser Technol. 45 (2012) 1–6. doi:10.1016/j.optlastec.2012.06.019.

[27] Y. Liao, C. Ye, D. Lin, S. Suslov, G.J. Cheng, Deformation induced martensite in NiTi and its shape memory effects generated by low temperature laser shock peening, J. Appl. Phys. 112 (2012). doi:10.1063/1.4742997.

[28] S.S. Mani Prabu, H.C. Madhu, C.S. Perugu, K. Akash, P. Ajay Kumar, S. V. Kailas, M. Anbarasu, I.A. Palani, Microstructure, mechanical properties and shape memory behaviour of friction stir welded nitinol, Mater. Sci. Eng. A. 693 (2017) 233–236. doi:10.1016/j.msea.2017.03.101.

[29] B. Rosa, P. Mognol, J. Hascoët, Laser polishing of additive laser manufacturing surfaces, J. Laser Appl. 27 (2015) S29102. doi:10.2351/1.4906385.

[30] E. V Bordatchev, A.M.K. Hafiz, O.R. Tutunea-fatan, Performance of laser polishing in finishing of metallic surfaces, Int. J. Adv. Manuf. Technol. Vol.73 (2014) 35–52. doi:10.1007/s00170-014-5761-3.

[31] C.P. Ma, Y.C. Guan, W. Zhou, Laser polishing of additive manufactured Ti alloys, Opt. Lasers Eng. 93 (2017) 171–177.

[32] S. Marimuthu, A. Triantaphyllou, M. Antar, D. Wimpenny, H. Morton, M. Beard, International Journal of Machine Tools &

Manufacture Laser polishing of selective laser melted components, 95 (2015) 97–104.

[33] K.Y. Luo, X. Jing, J. Sheng, G.F. Sun, Z. Yan, J.Z. Lu, Characterization and analyses on micro-hardness, residual stress and microstructure in laser cladding coating of 316L stainless steel subjected to massive LSP treatment, J. Alloys Compd. 673 (2016) 158–169. doi:10.1016/j.jallcom.2016.02.266.